POLYPHOSPHOINOSITIDES IN ARTIFICIAL BILAYER LIPID MEMBRANES: THE NATURE OF THE Ca^{++}- GATED CONDUCTANCE OF LYSOTRIPHOSPHOINOSITIDE CHANNEL

Masahiro SOKABE

(Behavioral Engineering)

CONTENTS

POLYPHOSPHOINOSITIDES IN ARTIFICIAL BILAYER LIPID MEMBRANES: THE NATURE OF THE Ca^{++}-GATED CONDUCTANCE OF LYSOTRIPHOSPHOINOSITIDE CHANNEL

Masahiro SOKABE

S. 1 GENERAL INTRODUCTION

Inositol phospholipids and membrane ionic permeability
—TPI-ionophore hypothesis—

The change in membrane ionic permeability is one of the central theme in membrane biology, and its molecular mechanism is the greatest missing link in the stimulus-response coupling of excitable cells. Although a large number of experiments have been carried out, any key molecules which control the membrane permeability have not yet been identified. Recent studies, however, suggested that phosphorylation of certain membrane components might strongly relate to the increase in membrane ionic permeability (Greengard & Kebabian, 1974).

On the other hand, it is well known that inositol phospholipids show a rapid phosphorylation and dephosphorylation of their phosphate moieties during membrane excitation (reviewed by Michell, 1975, 1979 ; Hawthorn & White, 1975). Inositol phospholipids consist of three kinds of lipids, phosphatidylinositol (PI or MPI), phosphatidylinositol 4-phosphate (diphosphoinositide, DPI), and phosphatidylinositol 4, 5-bisphosphate (triphosphoinositide, TPI). The structure of these lipids are shown in Fig. 1. We will use here, the shorter names PI, DPI, and TPI together with PPI (polyphosphoinositides) which is the generic mame for DPI and TPI.

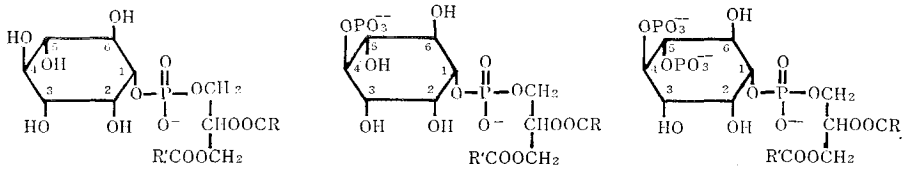

Fig. 1 Structure of inositol phopsholipids: (a)PI(MPI), (b)DPI, (c)TPI.
(modified from Michell, 1979)

PI is the major inositol lipid in most cells with much smaller quantities of DPI and TPI. The interconversion of these lipids is through ATP-dependent kinases and phosphomonoesterases as follows (modified from Kai & Hawthorn, 1969):

PI kinase

$PI + ATP \longrightarrow DPI + ADP$

DPI kinase

$DPI + ATP \longrightarrow TPI + ADP$

TPI phosphomonoesterase

$TPI + H_2O \longrightarrow DPI +$ inorganic phosphate

DPI phosphomonoesterase

$DPI + H_2O \longrightarrow PI +$ inorganic phosphate .

PPI, especially TPI has been speculated to have a key role in the control of ion permeation due to its unique bio and physicochemical properties as follows.

(1) Although TPI is a trace lipid in most eukaryotic cell, it is found in significant amounts in excitable tissues. Moreover, it is suggested to be concentrated at plasma membranes (Michell, 1979).

(2) It shows rapid turn over rate of its monoester phosphates, which may be increased with appropriate stimulation (Abdel-Latif et al., 1978 Birnberger et al., 1971; Brockerhoff & Ballou, 1961; Dawson, 1969; Tret'jak et al., 1977; Torda, 1974).

(3) It has an extraordinarily high affinity for Ca^{++} (Hendrickson, 1969), and shows hydrophilic-hydrophobic transition with Ca^{++} binding (Fig. 2). The affinity for Ca^{++} is significantly decreased with the hydrolysis of its monoester phosphates, thus in the order TPI> DPI> PI (Hendrickson & Reinertsen, 1971).

These properties together with the fact that Ca^{++} regulates the univalent cation permeability of nerve membranes led to the hypothesis that the interconversion of

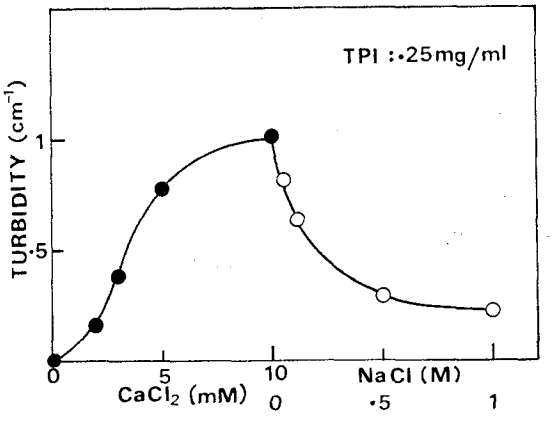

Fig. 2 Changes in the turbidity (at 350 mm) of TPI aqueous solution by successive addition of $CaCl_2$ (left hand side: closed circle) and of NaCl (right hand side: open circle). Ca^{++} increased the hydrophobicity of TPI, while Na^+ decreased it by releasing bound Ca^{++}. (modified from Sokabe, 1975)

these lipids may control the membrane ionic permeability via binding and release of Ca^{++} (Kai & Hawthorn, 1969; Hendrickson & Reinertsen, 1971, see Fig. 3). However, this hypothesis seems hardly to be tested directly on biological membranes because of its molecular complexity. So, we would propose here a simpler working hypothesis: "TPI may form an ionic channel of which conductance is regulated by Ca^{++}", which can be tested directly on artificial bilayer lipid membranes (Fig. 4). According to this

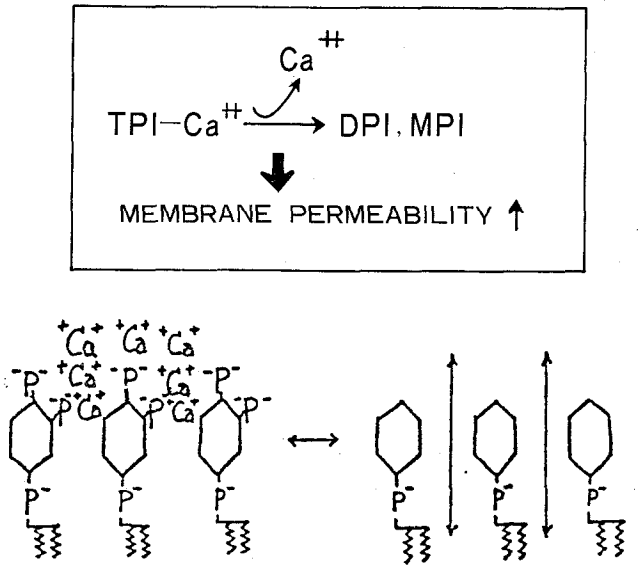

Fig. 3 Possible control of membrane permeability by PPI. Hydrolysis of TPI leads to open the channel by releasing bound Ca^{++}.
(modified from Kai & Hawthorn, 1969)

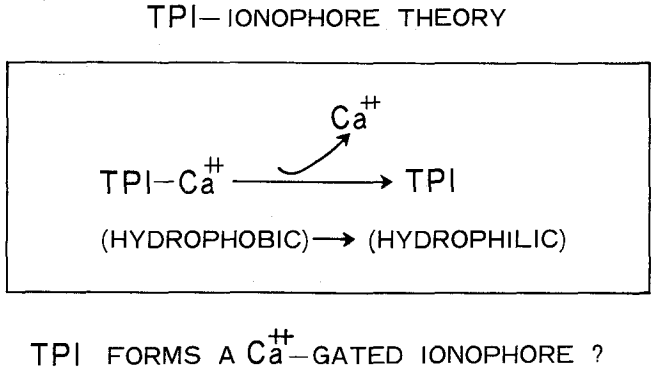

Fig. 4 Hypothesis for the Ca^{++}-gated channel made by TPI. Hydrophobic-hydrophilic change of TPI induced by the release of bound Ca^{++} leads to open the TPI-channel.

line, we tried to incorporate TPI into artificial bilayer lipid membranes. The intact TPI, however, had no effect on the membrane permeability, but trace amounts of lysoTPI an autoxidized product of TPI drastically decreased the membrane resistance by forming stable cationic channels.

We will present, in this report, a summary of our findings on this lysoTPI channel. In the next section, basic characteristics such as ion specificities and current-voltage characteristics of this channel are described. Main concern of this report is on the physcochemical mechanism of the Ca^{++}-effect on the univalent cation permeability of lysoTPI channel, which are closely described in Sec. 3 & 4. In the final section, based on our recent findings, some biological correlates of lysoTPI channel will be discussed.

S. 2 BASIC CHARACTERISTICS OF LYSOTPI CHANNEL

Here, after our previous works (Sokabe, 1975; Sokabe & Hayashi, 1978, Hayashi, Sokabe, Takagi, Hayashi & Kishimoto, 1978), the basic characteristics of lysoTPI channel such as (1) permeant ion specificity, (2) inhibitory ion specificity, and (3) current-voltage characteristics will be sunmarized.

a. Membrane formation and electrical measurement

Preparation of lysoTPI and membrane forming material (oxidized cholesterol) are described in the next section (S. 3. Matterials & Methods).

Membrane forming chamber is shown in Fig. 5 (2cm length, 6cm width, 2cm height).

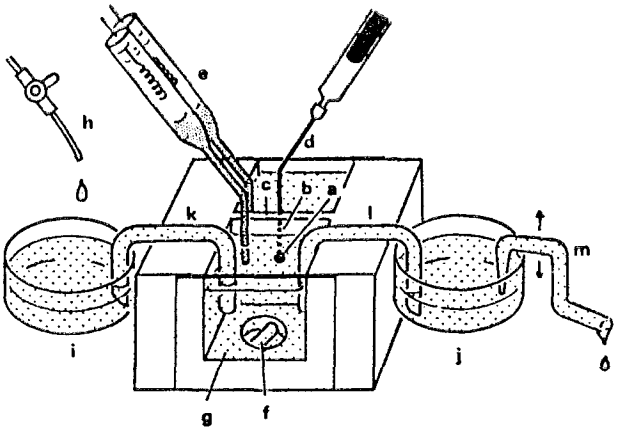

Fig. 5 Schematic diagram of apparatus for the formation of the membrane and for the perfusion of aqueous solution. a, membrane hole (1.3mm dia.); b, feeder hole (0.7mm dia.); c, septum (1.5 mm thickness); d, Teflon tube ; e, KCl/agar bridge and Ag/AgCl electrode; f, magnetic stirrer bar ;g, glass window; h, inlet of perfusing solution (Teflon tube with a stopcock); i and j, buffering vessel; k and l, siphon; m, level-controlling sliphon.

The chamber was made of Diflon blocks (Daikin Co. Ltd.) except for the glass windows attached to the front and back sides of the chamber. The chamber had vertical septum (1.5mm thickness) in which a membrane forming hole (1.3mm diameter) was located. An oil feeder hole (0; 7mm diameter) was drilled through the chamber septum to the membrane hole, this hole was connected to the syringe from which membrane forming oil was supplied. Two Teflon stirring bars were placed in each compartment (7ml volume), and siphon system was equipped for the perfusion of aqueous solutions.

After each chamber was filled with 5ml of 10mM Tris/Cl (pH 7.5), a thick biconcave lens of oxidized cholesterol solution was formed at the hole and was then sucked up to form a colored membrane, which spontaneously became a black membrane in a few minutes. lysoTPI and $CaCl_2$ were added to both compartments, then the membrane was incubated in this medium for 5minutes with gentle stirring. Under this condition, lysoTPI-Ca^{++} complex was incorporated into the black membrane to form ionic channels. If necessary, bulk solutions could be perfused with lysoTPI-free buffer to stop the successive incorporation of lysoTPI. A small quantities of concentrated solutions of electrolytes was added to either one or both bulk solutions in order to change the ionic composition.

The current-voltage curve of this modified membrane was linear provided that the applied voltage was less than 20mV (see Fig. 10). Therefore, zero current conductance of the membrane was obtained by applying a 10 mV rectangular voltage of 0.5 sec duration and by measuring the corresponding current using a low drift FET-top operational amplifier (Teledyne-Philblick, 1023). An A_g/A_gCl electrode was employed for electrcal measurement. It made contact with the saturated KCl solution in the shank of the glass tube which was connected to the aqueous phase of the chamber by means of a saturated KCl/agar bridge (see Fig. 5). The measurements were done at room temprature ($20\pm2°C$).

b. Permeant ion specificity

Upon addition of 10^{-6}g/ml lysoTPI and 1mM $CaCl_2$ in final concentration to both sides of a black membrane, the conductance gradually increased from $10^{-9}S/cm^{-2}$ to about $10^{-6}S/cm^{-2}$ within 5 minutes (Fig. 6a). However, no further increase in conductance was found by the subsequent addition of $CaCl_2$ (lower curve in Fig. 6b). The next great step of conductance increase was observed when a small aliquot of a concentrated solution of uni-univalent electrolyte was added both aqueous phases (indicated by arrows in Fig. 6a). The conductance was proportional to about the second power of the concentration of uni-univalent electrolyte (upper curve in Fig. 6b).

In order to know the species of ion which could permeate this membrane, potentials generated by KCl gradient across the membrane were measured. As shown in Fig. 7, the membrane potential could be fitted with the Goldman equation, if ratio of the

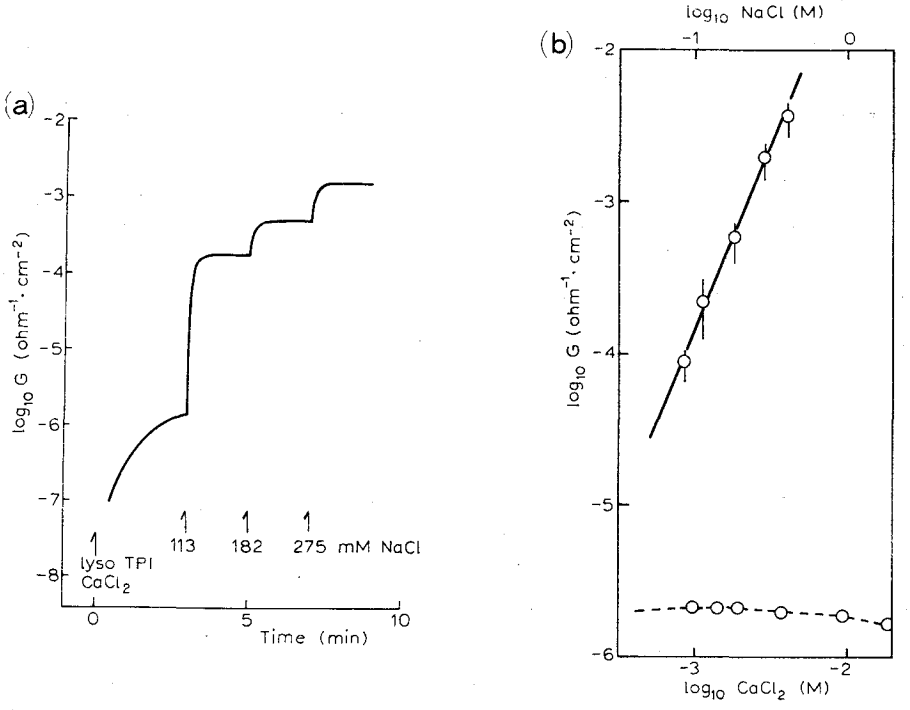

Fig. 6a. Time course of the membrane conductancc change of a black membrane modified with 10^{-6} g/ml lysoTPI and 1 mM $CaCl_2$. The first arrow indicates the time at which lysoTPI and $CaCl_2$ were added both the aqueous phases containing 10 mM Tris/Cl (pH 7.5). Aliquots (100 μl) of 2 M NaCl were added to both aqueous phases. Final concentrutions are indicated in the figure.

Fig. 6b. Plot of membrane conductance vs. concentration of electrolyte solution. Upper curve was obtained when the concentration of NaCl was increased in the presence of 1 mM $CaCl_2$. Lower curve was obtained when the concentration of $CaCl_2$ was increased in the absence of group IA cation. The data represent mean values ($\pm$S. D.) of at least four membranes.

permeability coefficient (P_{Cl^-}/P_{K^+}) was assumed to be 0.03. On the other hand, a concentration gradient of $CaCl_2$ generated no membrane potential. These results consistently implied that the membrane modified with lysoTPI was highly selectively permeable to the univalent cation, and was scarcely permeable to both Ca^{++} and Cl^-. Selectivity sequence among IA-cations was also measured. In the early paper (Hayashi et al., 1978), the sequence $Rb^+>Cs^+>Na^+>K^+>Li^+$ was reported. However, the sequence seemed to be changed with the lipid composition of bilayer lipid membranes (Hayasi & Sokabe, 1978). Our recent results showed that the most frequent sequence was $K^+>Rb^+>Cs^+>Na^+>Li^+$, which was similar to that of the K^+-channel in spuid axon (Hagiwara et al., 1972).

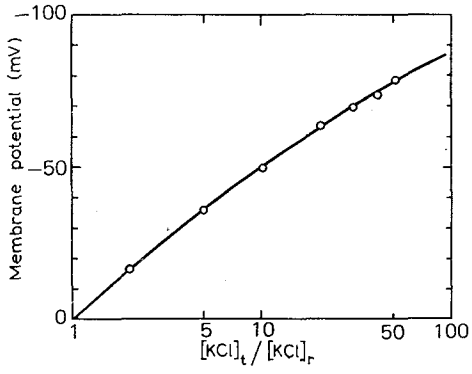

Fig. 7 Membrane potential generated by the concentration gradient of KCl. The concentration of KCl at the reference side was fixed at 8 mM. The subscripts "t" and "r" represent the two aqueous phases separated by the membrane (test and reference side). The solid line indicates the membrane potential calculated from the Goldman equation by assuming $P_{Cl^-}/P_{K^+}=0.03$

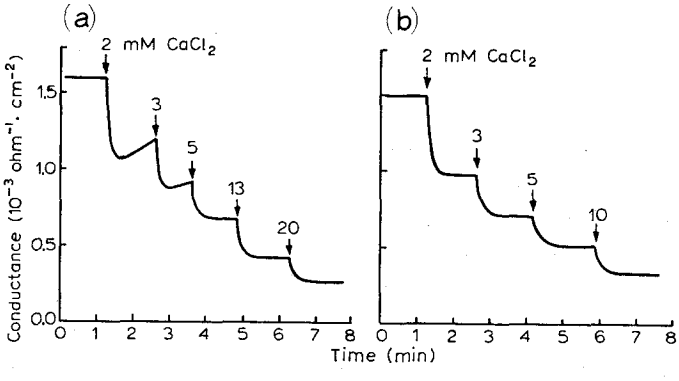

Fig. 8. Time course of the membrane conductance when $CaCl_2$ was added to one side of compartment (a) in the presence and (b) in the absence of lysoTPI. Both aqueous phases contained initially 10^{-6} g/ml lysoTPI, 1 mM $CaCl_2$, 275 mM NaCl and 10 mM Tris/Cl (pH 7.5). In the case (b), the aqueous phase was perfused with the lysoTPI-free solution containing same salt contents, and then 10 μl aliquots of 500 mM $CaCl_2$ were added successively to one side through a micropipette at the time indicated.

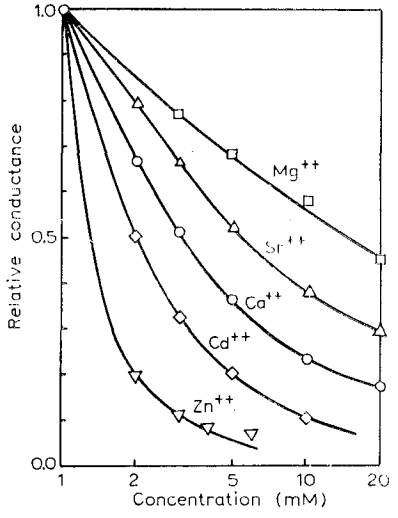

Fig. 9. Plot of relative conductance vs. concentration of divalent cation added to one side. Both aqueous phases contained initially 1 mM $CaCl_2$, 275 mM NaCl and 10 mM Tris/Cl (pH 7.5). The 10 μl aliquots of 500 mM solution of divalent cation were added to the test side after the perfusion.

c. Inhibitory ion specificity

The univalent cation conductance was greatly influenced by Ca^{++} or other divalent cations. Fig. 8 shows the change in membrane conductance when $CaCl_2$ was added to one side in the presence (a) and in the absence (b) of lysoTPI in the aqueous solutions. As shown in Fig. 8a, the Ca^{++}-effect has two aspects. The one is a rapid decrease just after the addition of Ca^{++}, and the other is a subsequent gradual increase. Since the latter effect was disappeared when lysoTPI was washed away by perfusion, it might reflect the additional incorporation of lysoTPI from aqueous solution because of a change in the hydrophobicity of lysoTPI-Ca^{++} complex. The former inhibitory effect seemed highly interesting, because, in nerve membranes, Ca^{++} was believed to control the univalent cation permeation. Therefore, we focused on this phenomena, which will closely be investigated in the succeeding sections. Though divalent cations other than Ca^{++} also inhibited the univalent cation permeation, their effectiveness differed as shown in Fig. 9. This implied that the inhibitory effect was not primarily ascribed to a simple electrostatic interaction such as screening effect.

d. Current-voltage characteristics

Above discussions were around zero current conductance i. e., equilibrium state of lysoTPI channel. In stationary state, lysoTPI showed another interesting behavior. Although, at symmetrical ionic condition, the I-V curves were nearly linear

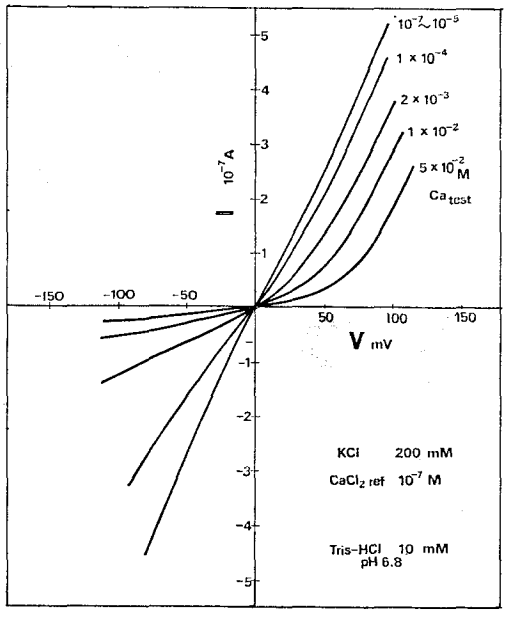

Fig. 10. Steady-state current-voltage characteristics of the membranes modified with lysoTPI at asymmetrical Ca^{++} condition. Increase in the Ca^{++} concentration in the test side led to strong current rectifications i. e., current from test side was inhibited.

i. e., the conductance was voltage independent, strong current rectification was observed at asymmetrical ionic condition.

Under the condition of Ca^{++}-asymmetry, the current from Ca^{++} concentrated side was extremely smaller than that from the opposite side. In another word, the conductance became voltage dependent through Ca^{++}-asymmetry. This effect was increased with the Ca^{++}-asymmetry (Fig. 10). K^+-asymmetry also induced similar effect at 1mM $CaCl_2$ (Fig. 11a), but the rectification was diminished at low Ca^{++} concentration (Fig. 11b.). This implied that the rectification induced by K^+-asymmetry did not arise from permeant ion asymmetry. Since it is suggested that relatively high concentration of K^+ could displace bound Ca^{++} from TPI (see Fig. 2), the rectification under K^+-asymmetry possibly originated from the asymmetry of bound Ca^{++}. Thus, K^+ was suggested to be not only a permeant ion but a conductance regulator through a competitive interaction with Ca^{++}. This idea will be tested by computer simulation in the next section.

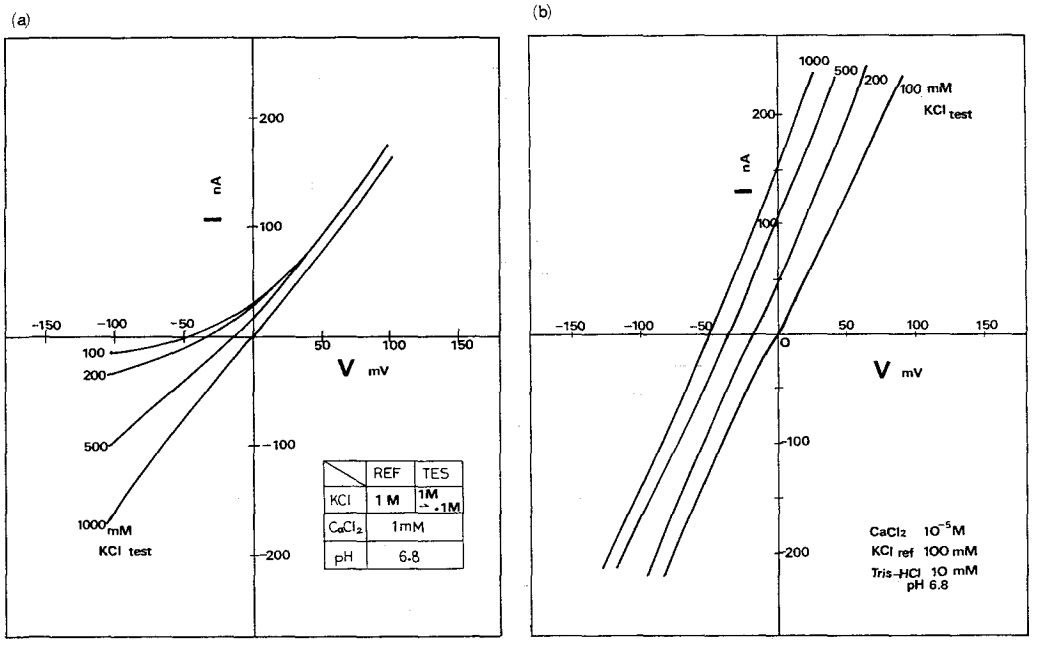

Fig. 11. Current- voltage characteristics of the membranes modified with lysoTPI at asymmetrical K^+ conditions in the presence of relatively high concentration of Ca^{++} (a) and low concentration of Ca^{++} (b). These curves suggest that the current rectification mainly arised from the asymmetry of bound Ca^{++}.

S. 3 Ca^{++}-EFFECT ON THE K^+-CONDUCTANCE OF LYSOTPI CHANNEL (I) —A MACROSCOPIC STUDY—

3.1 Introduction

a. Ca^{++}-effect on the ion permeation in biological membranes

It has strongly been suggested that Ca^{++} plays an important role in the regulation of ionic permeability of biological membranes. The sodium conductance of nerve membrane is reduced by Ca^{++} (Frankenhaeuser & Hodgkin, 1957). Several investigators have suggested that nicotinic acetylcholine-sensitive ionophore is blocked by Ca^{++} in a resting state (Neuman, 1973; Nachmanson & Neuman, 1975). Recently, it was demonstrated that sarcoplasmic reticulum membrane preparation induced a Ca^{++}-sensitive K^+ permeability on artificial bilayer membranes (Miller, 1978). Channel blocking by Ca^{++} was also demonstrated in the gap junction of a certain epithelial cell (Oiveira-Castro & Loewenstein, 1971; Rose et al., 1977).

b. Two hypotheses for the Ca^{++}-effect

Two kinds of hypotheses have been proposed for these Ca^{++}-effect on membranes. The first hypothesis concerning surface potential is based on the fact that Ca^{++} or

other divalent cations decrease the surface potential by screening the negative charges on the membranes. McLaughlin et al. clearly demonstrated that the magnitude of the surface potential of artificial bilayer membranes could be estimated by monitoring the neutral carrier mediated membrane conductance (McLaughlin, et al., 1970, 1971). Although the surface potential hypothesis well predicted the Ca^{++}-effect such as G-V shift in nerve membranes (Gilbert & Ehrenstein, 1969), this hypothesis could not explain the whole aspects of Ca^{++}-effect on nerve membranes (Gotoh, 1975). Indeed, the Ca^{++}-effect that could not be attributed to the screening effect was reported (Miller, 1978).

The second hypothesis is based on the idea that Ca^{++} itself behaves as a gate for univalent cation channel (Gotoh, 1957), or as an effector of channel gating substance (Fishman, et al., 1971). At present, however, such a Ca^{++}-sensitive channel substance has not been identified. Even an appropriate model substance for the physicochemical study of such a Ca^{++}-effect has not been proposed. Although the univalent cation conductance of gramicidin A channel was depressed by divalent cations (Hladky & Haydon, 1972; Bamberg & Läuger, 1977), the efficiency of Ca^{++} was relatively weak, i. e., conductance depression required relatively high concentration of divalent cation (10^{-1}-1M). In this respect, gramicidine A seems inadequate for the model substance to investigate the Ca^{++}-effect from physiological point of view.

It has been shown, in the previous section, that lysoTPI could induce a univalent cation conductane that was profoundly depressed by Ca^{++} in artificial bilayer membranes. Since the polar head group of TPI reveals a high affinity for Ca^{++} in the same magnitude as EDTA (Hendrickson & Fullington, 1965), lysoTPI is expected to keep such a property for divalent cations. We found that the efficiency of divalent cations to reduce the membrane conductance was considerably different to one aother (see Fig. 9). Therefore, the Ca^{++}-effect in this system was expected to be primarily due to specific binding to the head group of lysoTPI.

In this section, in order to know the detaied mechanism of Ca^{++}-effect on lysoTPI channel, we examined the zero current conductance of the modified bilayers in wide concentration range of K^+ and Ca^{++}. The change in membrane conductance was mainly explained by a cation exchange model, where it was assumed that K^+ was not only a permeant ion but an activator for the channel and that Ca^{++} was a competitive inhivitor to K^+.

Most of the contents in this section are described after our recent work (Sokabe & Hayashi, 1981a).

3.2 Materials and Methods

a. Preparation of lysoTPI

lysoTPI was obtained by autoxidation of TPI as previously reported (Hayashi et al., 1978). TPI was purified from Folch fraction of bovine brain by the method of Hendrickson

and Ballou (1964). The concentrated aqueous solution of TPI (3–5mg/ml) was exposed to ultra-violet light (2537 Å in wave length) for a week in a qualtz cell. Autoxidized-TPI was applied on DEAE-cellulose (Whatman DE-32) column and eluted with 0.3 M CH_3COONH_4 in chloroform/methanol/water (20 : 9 :1). Eluate was evapolated and lyophilized, and the dried material was washed free of salt by 2-phase system which was composed of $CHCl_3$/CH_3OH/1N · HCl (2 : 1 : 0.6). Lower phase was neutralized by conc. NH_4OH and evapolated to dryness. Obtained material gave a single spot on oxalate-impregnated silica gel 60HPTLC plate (Jolles et al., 1979) when it was de-evloped with chloroform/acetone/methanol/acetic acid/water (40 : 15 : 13 : 12 : 8).

With the aim of characterizing this sample the molar ratio of ester fatty acid to phosphorus was determined. The fatty acid ester was determined by the method of Snyder et al. (1959) and the phosphorus was determined by the method of Bartlett (1959). It was found that the sample contained one fatty acid ester per three phosphorus residues. This result implied that TPI molecules were completely oxidized and broken down into lysoTPI molecules.

Purified lysoTPI caused the same phenomena in bilayer membranes as those induced by autoxidized-TPI not purified, although the latter sample contained free fatty acids or lipidperoxides. Most of the results in this report were obtained by using the crude sample.

b. Preparation of oxidized cholesterol

Oxidized cholesterol was obtained by the method of Robinson and Strickholm (1978). A solution of 4% (W/V) cholesterol (99% pure, Sigma Chemical Co. Ltd.) in 25 ml of 1 : 1-mixture of n-decane and n-tetradecane was refluxed in oxygen atmosphere for 1.5h. Molecular oxygen (Seitetsu Kagaku, Zero-A) was bubbled into the flask (50 ml) equipped with Dimroth-type condenser at the rate of 4–5 ml/min. Obtained material was cooled for over night at 4°C and the supernatant was for use.

The glass wares used in this preparation were cleaned by the following procedure. They were boiled in detergent cleaner and rinsed with tap water for 1 h and then soaked in $KMnO_4$-H_2SO_4 for 24 hrs and rinsed with distilled water for 1 hr. They were again rinsed with double distilled water and dried in oven.

The alkanes were purchased from Tokyo Kasei Co. and passed through active alumina for use.

c. Membrane formation

In order to perfuse aqueous solutions in a stable and simple manner, the apparatus shown in Fig. 12 was developed. This apparatus consists of three main parts made of Daiflon (trifluoromonochloroethylene; purchased from Daikin Engineering Co. Ltd.). The first part was a partition (0.2 mm in thickness) containing a hole (1.3 mm in diameter) in its center. Two compartments made of Daiflon were separated by the partition. The volume of each compartment was approx. 0.3 ml. The front compartment had a

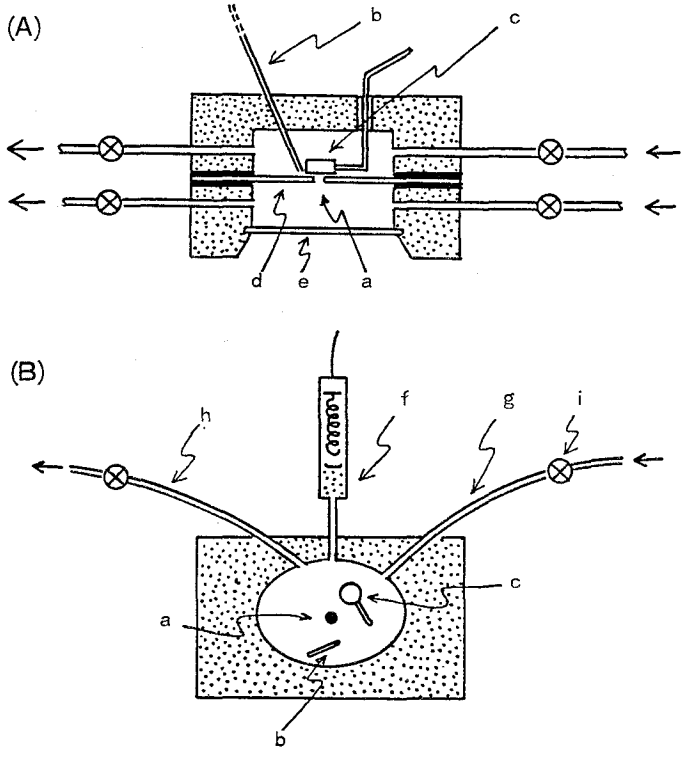

Fig. 12. Schematic diagram of experimental apparatus for the formation of bilayers and for the perfusion of bulk solutions (A, top view; B, front view): a, membrane hole (1.3 mm dia.); b, feeder tube; c, Daiflon blush; d, septum; e, glass window; f, KCl-agar bridge and Ag-AgCl electrode; g, inlet Teflon tube; h, outlet Teflon tube; i, stop cock.

glass window through which one could observe the membrane. The back compartment was equipped with a Teflon-coated stainless pipe connected to microsyringe which supplied the membrane forming material. The back compartment was also equipped with a Daiflon brush which could be manipulated from out side. These three parts were attached tightly with metal screws and fluorine-contained rubber was used as a packing. Oxidized cholesterol solution having been supplied to the membrane hole, bilayer membrane was formed by a stroke of the brush.

Each compartment was perfused with arbitrary solutions through two Teflon tubes (2 mm in diameter). When the stop cocks of one compartment were closed, the opposite compartment could be safely perfused with arbitrary solutions without destroying the membranes. We could change the solution within 30 sec. After the modification of bilayer membranes with lysoTPI (10^{-6}g · ml^{-1}) and $CaCl_2$ (1 mM), the solutions were washed out by perfusion in order to eliminate the successive adsorption

of lysoTPI to the membrane.

All of the perfusing solutions were buffered with 10 mM Tris-HCl (pH 7.2). KCl and $CaCl_2$ were the special grade of Wako Chemical Co. Double distilled water was used.

In the $CaCl_2$ concentration range below 10^{-7} M, we used Ca^{++}-buffer (1 mM EGTA). In this case, 20 mM Tris-maliate (pH 6.8) was employed as a pH buffer.

Electrical measurements were basically the same as described before (see S. 2a).

All experiments were done at room temperature (23±2°C).

3.3 Results and Discussion

a. Dependency of the membrane conductance on K^+ and Ca^{++} concentration

The membrane conductance was dependent on both K^+ and Ca^{++} concentrations. Fig. 13 indicates the dependency of the conductance on KCl concentration in the presence of various concentrations of $CaCl_2$. Membranes were placed under symmetrical condition.

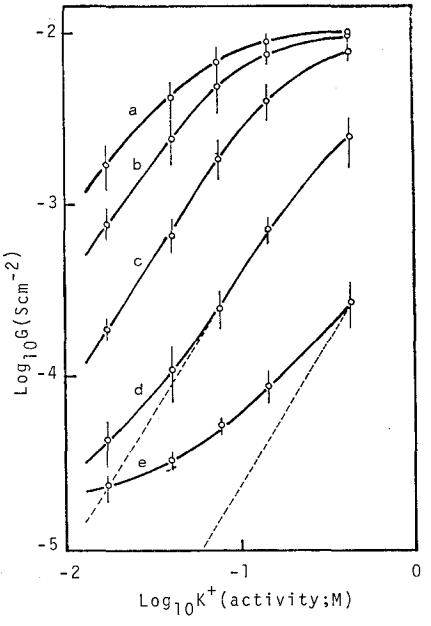

Fig. 13. Double logarithmic plot of the membrane conductance vs. activity of KCl in the presence of various concentrations of $CaCl_2$: a, 10^{-6} M; b, 10^{-5} M; c, 10^{-4} M; d, 10^{-3} M; e, 10^{-2} M. Dashed lines indicate intrinsic potassium conductance obtained by the subtraction of leaky conductance (the membrane conductance in the absence of KCl) from the apparent conductance. The data represent mean values (±S. D.) of at least four membranes.

At first, membrane conductance in very low Ca^{++} concentration range will be discussed. Membrane conductance was independent of Ca^{++} concentration in the range below 10^{-6}M. However, the membrane conductance increased with the increase in K^+ concentration (see most upper curve in Fig. 13). This conductance increase might be explained from two aspects. One aspect was the increase in the conductance of individual single channels. Another one was the increase in the number of open channel with K^+ concentration, i. e., K^+ is not only a current carrier but a channel activator as has been proposed for lysolecithin channel (Lee & Chan, 1977). In our preliminary experiments (see Fig. 19), it was found that the single channel conductance (approx. 6 pS in the presence of 500 mM KCl) of lysoTPI was dependent on K^+ concentration though the dependency was weak comparing with that observed in the many-channel membranes. That is, a ten-fold increase in KCl concentration (50–500 mM) caused approx. 1.5-fold increase in the single channel conductance of lysoTPI (see Fig. 21), while it caused a 2.5-fold increase in the conductance of many-channel membranes. The single channel conductance saturated at approx. 200 mM KCl while the membrane conductance became saturated at approx. 500 mM KCl in the absence of Ca^{++}. Therefore, the conductance increase in the absence of Ca^{++} was not only due to the increase in the single channel conductance but partly due to the increase in the number of open channels.

The lowest curve in Fig. 13 deviated from the line of slope 2 indicating that there was a leaky current which was independent of K^+-concentration. We previously reported that $CaCl_2$ caused a small conductance (approx. 10^{-6}–10^{-5} S. cm^{-2}) on bilayer membranes modified with lysoTPI. This conductance elicited by $CaCl_2$ was nearly constant in the $CaCl_2$ concentration range beyond 10^{-3} M. The leaky conductance above mentioned was expected to be identical to the conductance by $CaCl_2$. The broken lines in Fig. 13 indicate intrinsic K^+-conductance which was calculated by the subtraction of the leaky conductance from the apparent membrane conductance. The slope of these broken lines were approx. 2.

Thus, in the presence of Ca^{++}, membrane conductance was proportional to about the second power of the concentration of KCl. K^+ and Ca^{++} affected the membrane conductance in antagonistic manner. Relatively small amount of Ca^{++} inhibited the K^+-conductance. On the other hand, the addition of an excess of EGTA to the bathing solutions containing Ca^{++} brought about an increase in K^+-conductance. Moreover, the conductance change could not be ascribed to the change in the surface potential as will be discussed later. Therefore, it was suggested that cation exchange reaction which caused an activation and inactivation of the channel underlay in the conductance change of the membrane modified with lysoTPI.

In order to investigate the mechanism for the depression of K^+-conductance by Ca^{++}, several data shown in Fig. 13 were replotted into double reciplocal plot:

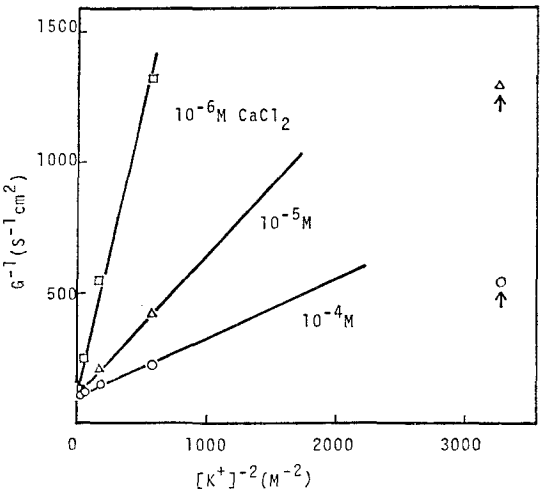

Fig. 14. Double reciprocal plot of the membrane conductance vs. $[KCl]^2$. Data were replotted from the mean values indicated in Fig. 13: -○-, 10^{-6} M $CaCl_2$; -△-, 10^{-5} M; -□-, 10^{-4} M. The data gave straight lines crossing a common intersect indicating that Ca^{++} was a competitive inhitor of the K^+-conductance. In low K^+ concentration, however, the data deviated from the straight line as indicated by vertical arrows. These deviations could be explained in terms of a negative surface potential that was effective only in low ionic concentration region as discussed later.

(membrane conductance)$^{-1}$ vs $[K^+]^{-2}$. As shown in Fig. 14, the data gave straight lines crossing a common intersect. It was suggested that two potassium ions were necessary for the activation of one channel and that Ca^{++} was a competitive inhibitor of the K^+-conductance. Since the single channel conductance of lysoTPI revealed constant irrespective of the presence or absence of Ca^{++} (see Fig. 22), the conductance in the presence of Ca^{++} seems to be ascribed mainly to the increase in the number of conducting channel rather than the increase in the single channel conductance.

b. Independency of the Ca^{++}-effect on each side of the membrane and half pore hypothesis

Fig. 15 shows the Log-Log plots of the relative membrane conductance vs. Ca^{++} concentration in Ca^{++}concentration range above 1 mM. When the Ca^{++} concentration of both bathing solutions were changed at the same time, the plot gave a straight line of which slope was approx. 1. On the other hand, when the Ca^{++} concentration of only one side of the membrane was changed, the plot gave a straight line of which slope was approx. 0.5 (see upper line in Fig. 15). The relative conductance at

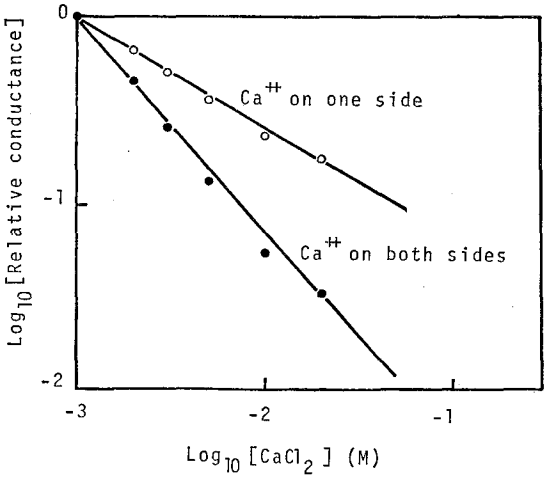

Fig. 15. Double logarismic plots of relative conductance vs. [$CaCl_2$]: the relative conductance was obtained by dividing the membrane conductance by that at the initial condition (1mM Ca^{++}). -o- indicates the relative conductance when the Ca^{++} concentration of one side of the membrane was successively changed with a constant Ca^{++} concentration on the other side (asymmetric condition). -●- indicates the relative conductance when the Ca^{++} concentration of both aqueous phases were changed (symmetric condition). Data were well fitted by two straight lines of which slopes were -0.58 and -1.16, respectively.

symmetrical Ca^{++}-condition was obtained by the square of that at asymmetrical Ca^{++}-condition. Thus, it was suggested that the Ca^{++}-effect on each surface of the membrane was statistically independent each other.

In order to induce univalent cation conductance to lipid bilayers, it was necessary that lysoTPI presented on both sides of the membrane. This fact suggests that lysoTPI formed half pores on each side of the membrane as has been supposed for nystatin and amphotericin B (Finkelstein & Holz, 1973). Taking into account of this hypothesis and the independency of Ca^{++}-effect, Ca^{++} is expected to gate or block only the half pore on the same side of the membrane, and the membrane conductance may be proportional to the fraction of the open (active) state half pores on each side of the membrane.

c. Examination of surface potential

We examined the surface potential of the modified membrane by using neutral carriers, i. e., nonactin and valinomycin as a surface potential probe. McLaughlin et al. (1970, 1971) reported that the membrane conductance brought about by the addition of neutral carrier was a good indicator of the surfale potential of the membrane. The

carrier mediated membrane conductance of a charged bilayer (G^c) is equal to that of a neutral bilayer (G^n) times the exponent of the surface potential ($\psi(0)$) (McLaughlin et al., 1970, 1971) :

$$G^c = G^n \exp(-F\psi(0)/RT) \quad (1)$$

where F/RT is a usual meaning.

There was a slight difference between carrier-mediated conductance for the membranes modified with lysoTPI and that for the intact oxidized cholesterol membranes except for low electrolyte concentration range. In the presence of $CaCl_2$ above 1 mM, G^c was equal to G^n, but below 1 mM $CaCl_2$, G^c was gradually increased with the decrease in $CaCl_2$ concentration and saturated at about 10^{-6} M $CaCl_2$. In the presence of 10^{-7} M $CaCl_2$ and 20 mM NaCl, G^c for nonactin was approx. 2.5 times greater than G^n. Furthermore, since G^c for valinomycin in the presence of 10^{-7} M $CaCl_2$ and 20 mM KCl was approx. 2 times greater than G^n, the initial surface potential of the modified membrarane might be evaluated about -20 mV at 22°C.

When the Ca^{++} concentration was changed from 10^{-7} to 10^{-3} M, lysoTPI mediated membrane conductance was depressed to 1/20 of original value. Taking into account of the dependency of the membrane conductance on KCl shown in Fig. 13, such a large conductance depression by Ca^{++} could not be attributed to the decrease in the surface potential by Ca^{++}. Indeed, above 1 mM Ca^{++}, where there was no surface potential, a profound conductance depression by Ca^{++} was still observed (see Fig. 15). These findings strongly suggested that the conductance depression by Ca^{++} arised from a more direct action of Ca^{++} to lysoTPI channel. Although the underlying mechanism of the interaction between Ca^{++} and the channel has been obscure, a preliminary phenomenological model for the conductance depression by Ca^{++} will be discussed in the following section.

d. A model

Fundamental characteristics of the K^+-conductance and several assumptions will be summarized here before making a model for the K^+-conductance depression by Ca^{++}.

(1) To induce a membrane conductance, it was necessary to add lysoTPI to the both bathing solutions, this suggested that lysoTPI made so called "half pores" (Finkelstein & Holz, 1973) on the membrane surface. It was expected that the two half-pores on the opposite side of the membrane associated to make a complete channel which spanned the bilayer.

(2) The incorporation of lysoTPI into bilayers seemed irreversible because the membrane conductance remained constant even after the removal of lysoTPI from aqueous solutions by perfusion. lysoTPI channel, once formed, was hold stably in bilayer, namely the number of the channel was kept constant during experiment on

one membrane. Owing this and (4), the possibility for the drop out of the channel from membrane or successive incorporation of the channel from aqueous phases with the change of ionic concentration could be precluded, and the reaction under discussion must be restricted on the membrane.

(3) The current carrier of this system was univalent cation, neither divalent cation nor anion, because the membrane conductance elicited by $CaCl_2$ was by several orders less than the univalent cation conductance, and because no membrane potential was generated by Ca^{++} or anionic concentration gradient (see S. 2b).

(4) Since the membrane conductance was dependent only on the electrolyte concentration, not on the sequence of the perfusion, the reactions between the channel and K^+ or Ca^{++} were completely reversible.

(5) Membrane conductance must be proportional to $[Ca^{++}]^1$ in high Ca^{++} concentration range and to $[K^+]^2$ in relatively low K^+ concentration range. K^+-conductance attained to a maximum level in high K^+ concentration range. It was assumed that K^+ was not only a permeant ion but an activator of the channel because the change in membrane conductance with K^+ concentration could not be explained by the dependency of the single channel conductance on K^+ concentration. Channel gating was assumed to be employed by uni- and divalent cation exchange at the orifice of the channel.

(6) It was also assumed that Ca^{++} was an inhibitor which gated the channel in all-or-none fashion and that the gating processes of the half-pores on both sides of the membrane were independent each other.

(7) The surface potential of the modified membrane was negligibly small except for a low ionic concentration region.

(8) All processes under discussion were assumed to be in an equilibrium state because we were dealing with the zero current membrane conductance.

Reaction on one side of the membrane was assumed to be described as follows:

$$S+2M^+ \rightleftharpoons S_m\ ;\ K_1=[S_m]/[S][M^+]^2\ , \qquad (2\text{-a})$$

$$S+C^{++} \rightleftharpoons S_c\ ;\ K_2=[S_c]/[S][C^{++}]\ , \qquad (2\text{-b})$$

$$[S_t]=[S]+[S_m]+[S_c] \qquad (2\text{-c})$$

where S denotes a free-state of cation binding site, S_m denotes a univalent cation-bound state and S_c denotes a divalent cation-bound state of the binding site. K_1 and K_2 are inverse of dissociation constants of S_m and S_c, respectively. [ ] denotes the concentration (activity) or density of the material bracketted at membrane surface. $[S_t]$ is a total density of the binding site which is constant during our experiments. S_m is assumed to contribute to the membrane conductance. $[S_m]$ can be given from Eqs. (2-a, b, c).

$$[S_m]=\frac{K_1[M^+]^2[S_t]}{1+K_1[M^+]^2+K_2[C^{++}]} \quad . \tag{3}$$

Membrane conductance (G) will be proportional to the density of conducting channel ([P]) which is proportional to the product of the density of the K^+-bound half-pore ([Ph]) on each surface of the membrane. That is,

$$G=\Lambda[P]=\Lambda K_3[Ph]_{cis}[Ph]_{trans} \tag{4}$$

where Λ is a single channel conductance and K_3 is an association constant between the half pores on opposite side of the membrane. $[Ph]_{cis}$ and $[Ph]_{trans}$ are the density of the half-pore on cis- and trans-side, respectively.

From our experimental results, it was suggested that G was proportional to $[M^+]^2*[C^{++}]^{-1}$ in relatively high concentration of Ca^{++}. Under symmetrical electrolyte condition, G is proportional to $[Ph]^2$ as predicted from Eq. (4), where $[Ph]=[Ph]_{cis}=[Ph]_{trans}$. Therefore, the density of the univalent cation-bound half pore on one side of the membrane must be proportional to $[M^+][C^{++}]^{-1/2}$. Following assumption will make our hypothesis consistent. That is, S_{mcis} generates two half-pores on cis side of the membrane,

$$S_{mcis} \rightleftharpoons Ph_{cis}+Ph_{cis}\,; \quad K_4=[Ph]^2_{cis}/[S_m] \tag{5}$$

where K_4 denotes the dissociation constant of S_m to half pore. $[Ph]_{cis}$ can be described as

$$[Ph]_{cis}=(K_4[S_m]_{cis})^{1/2}. \tag{6}$$

Erom Eqs. (3), (4) and (6), membrane conductance (G) can be described as

$$G=\frac{\Lambda K_4K_3K_1\ [M^+]^2[S_t]}{1+K_1[M^+]^2+K_2[C^{++}]} \quad . \tag{7}$$

The contribution of the surface potential to the membrane conductance was considered, since surface potential of the modified membrane was not negligible in low Ca^{++} concentration range.

Cation concentration at the membrane surface, $[C^{+2}]$ can be shown to be equal to the concentration in the bulk solution times the exponent of the potential at the surface of the membrane, $\psi(0)$:

$$[C^{+z}]=[C^{+z}]_b \exp\ (-ZF\psi(0)/RT)=[C^{+z}]_b * f^z \qquad (8)$$

where z is the valency of the cation, $[C^{+z}]_b$ is the concentration in the bulk solution, f is exp $(-F\psi(0)/RT)$, RT/F=23.5 mV at 22°C. Then Eq. (8) can be rewritten as

$$G=\frac{AK_4K_3K_1[S_t][M^+]_b^2\ f^2}{1+K_1[M^+]_b^2\ f^2+K_2[C^{++}]_b\ f^2} \qquad (9)$$

Because the exact curve of A as a function of K^+-concentration was not determined, and the values for $[S_t]$, K_3, and K_4 were unknown, we calculated relative conductance (Eq. 10) instead of eq. (9).

Relative conductance can be defined:

$$G'/G=\frac{1+K_1[M^+]_b^2\ f^2+K_2[C^{++}]_b\ f^2}{1+K_1[M^+]'^2_b\ f'^2+K_2[C^{++}]'_b\ f'^2} * \frac{[M^+]'^2_b\ f'^2}{[M^+]_b^2\ f^2} \qquad (10)$$

where f′ denotes the Boltzmann factor corresponding to the surface potential which arised in the condition defined by $[M^+]'_b$ and $[C^{++}]_b'$. The method for the calculation of the Boltzman factor is described in APPENDIX

e. Evaluation of the model

Fig. 16 indicates the dependency of the relative conductance on Ca^{++} concentration in the presence of various concentrations of K^+. The data were replotted from Fig. 13. The curves were calculated from Eq. (10) as best fits for the data; $\sigma_{initial}=4.1\times$

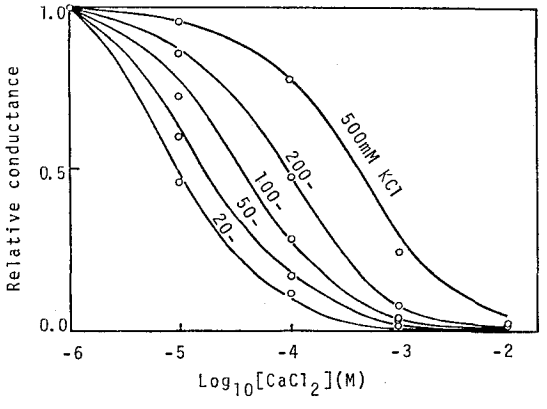

Fig. 16. Relative conductance vs. $CaCl_2$ concentration in the presence of various concentrations of KCl. Curves were calculated from Eq. (10). Initial charge density, $\sigma_{initial}=4.1\times10^{-4}$ Å^{-2}, $K_1=44$ M^{-2}, $K_2=21{,}000$ M^{-1}. The data represent the mean values calculated from Fig. 13.

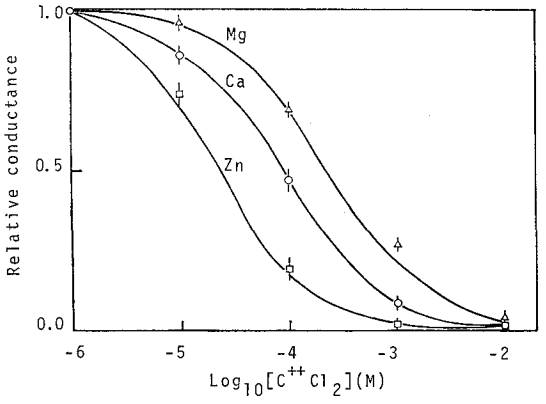

Figure 17. Plot of relative conductance vs. concentration of some divalent cations: -△-, Mg^{++}, -○-, Ca^{++}, -□-, Zn^{++}. The data represent the mean values (±SD) of at least two membranes. The curves were calculated from Eq. (10) with substituting the following values for K^2: Mg^{++}, 5,000 M^{-1}, Ca^{++}, 21,000 M^{-1}, Zn^{++}, 100,000 M^{-1}. The values for K_1 and $\sigma_{initial}$ are the same as those used in Fig. 16.

$10^{-4}Å^{-2}$, $K_1=44$ M^{-2}, $K_2=21,000$ M^{-1}, where $\sigma_{initial}$ denotes initial charge density of the modified membrane (see APPENDIX). If $\sigma_{initial}=0$ was assumed, the calculated curves at 20 mM and 50 mM KCl were nearly identical to that at 100 mM KCl. Therefore, the decrease in negative surface potential seems to contribute, in some degree, to the change in membrane conductance in low ionic concentration. Divalent cations other than Ca^{++} also affected the K^+-conductance as shown in Fig. 17. These data could also be explained in terms of Eq. (10) by using following association constants : $K_{Mg}=5,000$ M^{-1}, $K_{Ca}=21,000$ M^{-1}, $K_{Zn}=100,000$ M^{-1}. Thus the model could well predict the effect of other divalent cations on K^+-conductance with only changing the value for K_2.

As described before, neutral carrier experiments deduced that the surface potential in the presence of 10^{-6}M $CaCl_2$ and 20 mM KCl was approx. 20 mV. This value was in good agreement with that ($\psi(0)=-16.3$ mV) predicted from Eq. (10) when we tried to get the best fit of calculated curves to the experimental data (see APPENDIX). These results give a strong support for our model.

At present, although the precise physichochemical mechanism of the Ca^{++}-effect on K^+-conductance is unknown, the basic assumptions employed in the model might be correct. It is known that TPI combines Ca^{++} with high affinity, which causes a typical hydrophilic-hydrophorbic micelle transition (Hendrickson & Fullington, 1965; Sokabe, 1975). It is expected that Ca^{++} depressed the membrane conductance through specific binding to the head group of lysoTPI accompanying large increase in the hydrophobicity

of lyso TPI channel. Since Ca^{++} is known to change the micelle form of phospholipids and lysophospholipids (Cullis & Kruijff, 1979), it is also expected that a certain structural change of the channel was induced by Ca^{++}. Closer investigations of the Ca^{++}-effect on lysoTPI channel with single-channel experiment are described in the next section.

APPENDIX

Calculation of the surface potential

The Graham equation (Graham, 1947) from the theory of the diffuse double layer relates the surface potential to the charge density (σ) and the bulk aqueous concentration of monovalent and divalent ions ($[C_i]_b$) :

$$\sigma = [2\varepsilon\varepsilon' RT \sum_i [C_i]_b [\exp(-Z_i F \psi(0)/RT) - 1]]^{1/2} \quad \text{(A1)}$$

where ε is the dielectric constant of water and ε' is the permittivity of free space, and ψ (0) is the surface potential.

Negative surface charge on the membrane was expected to arise from lysoTPI adsorbed to the membrane. If a cation binding site (S) was assumed to have two negative charges, the charge density of the membrane should be proportional to the density of free-site ([S]) which was described in Eq. (1) :

$$\begin{aligned}\sigma &= 2[S]e \\ &= 2[S_t]e/(1 + K_1[M^+]^2 + K_2[C^{++}]) \end{aligned} \quad \text{(A2)}$$

where e denotes the elementary electric charge. Since the initial charge density ($\sigma_{initial}$) is equal to $2[S_t]e$,

$$\sigma = \sigma_{initial}/(1 + K_1[M^+]^2 + K_2[C^{++}]). \quad \text{(A3)}$$

Thus, combining (A1) and (A3) with substituting proper values for K_1, K_2 and $\sigma_{initial}$, we can get the value for the surface potential ($\psi(0)$).

S. 4 Ca^{++}-EFFECT ON THE K^+-CONDUCTANCE OF LYSOTPI CHANNEL (II)
—A MICROSCOPIC STUDY—

4.1 Introduction

Ca^{++}-effect on single channel conductance

One of the unique features of the membranes modified with lysoTPI lies in the fact that the divalent cations such as Ca^{++} strongly depressed the univalent cation conductance. It was expected that the conductance depression by Ca^{++} was due to specific

interaction between Ca^{++} and lysoTPI channel. Surface potential which is an important factor in the regulation of membrane ionic permeability did not seem to play an essential role in this system.

The first aim of the microscopic study is to verify the hypothesis that lysoTPI forms an ionic channel. The second aim is to see the effect of Ca^{++} on the single channel. The latter point seems of special interest if it were compared with the channel blocking of the gramicidin A for which the single channel conductance was gradedly reduced by the divalent cations such as Ca^{++} or Ba^{++} (Bamberg & Läuger, 1977).

In this study, we found that lysoTPI formed a pore like structure of which single channel conductance was not affected by Ca^{++} in both oxidized cholesterol and glycerylmonooleate bilayer membranes. Ca^{++} modified the dwell times for "open" and "closed" state of the lysoTPI channel as well as the transition frequency between these states. To our knowledge, this is the first finding that a certain phospholipid reveals a single channel behavior. Most of the contents in this section are described after our recent work (Sokabe & Hayashi, 1981 b).

4.2 Materials and Methods

a. Materials

Preparation of lysoTPI and oxidized cholestrol was the same as described in S. 3.2 a. Bilayer lipid membranes were formed from oxidized cholesterol or glycerylmonooleate.

Glycerylmonooleate (Sigma) was desolved in n-hexadecane (14 mg/ml) and used without further purification.

Alkanes were purchased from Tokyo Kansei Co. Ltd. and passed through active-alumina column.

b. Membrane formation and electrical measurement

Membrane forming apparatus and current measuring procedure were identical to those reported by Neher et al. (1978). (Fig. 18). Membranes were formed in a small hole (approx. 200 micrometer in diameter) on the wall of a 10 ml disposable polypropylen test-tube. The test-tube was doped in the solutions containing 1.6–2 nM of lysoTPI, 50–500 mM of KCl, 10^{-6}–10^{-2} M of $CaCl_2$ and 1 mM of Tris-HCl (pH 7.2) in a 50 ml glass beaker. When the many-channel experiment was done, 16–48 nM of lysoTPI was employed. Membrane forming materials were applied to the membrane hole with a glass micropipette. After thinning the membrane, current fluctuations were measured at constant voltage. Current amplifier connected through coaxial connector to the test-tube was constructed from an electrometer amplifier (Teledyne 1035–02) equipped with 10^{10} ohm glass enclosed resistor and 10 pF titanium capacitor in feedback circuit. With this configuration, the limited bandwidth and electrical noise of the measuring system (including membrane) were about 8Hz and lower than 50 fA, respectively. Ag-AgCl coiled electrodes were used. Most of the experiments

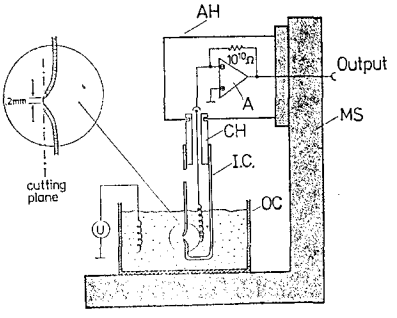

Fig. 18. Membrane formation apparatus for the single channel experiments. OC, outer chamber; IC, inner chamber; CH, chamber holder; A, amplifier; AH, amplifier headstage; MS, micromanipulator stand.
(Neher et al., 1978).

were carried out with applying ±50 mV dc-voltage (the inner side of the tube was difined as a virtual ground) through pulse generator (Nihon Koden, SEN 3101), and subsequent membrane current fluctuations were converted to voltage fluctuations (10 mV/1 pA) which were recorded by a low-speed pen recorder (National VP 6521A, limited bandwidth; 1 Hz), or high-speed pen recorder (Sanei, RECTIGRAPH-8S, limited bandwidth; 80 Hz) and then analized. The former recorder was used for the estimation of the magnitude of the single channel conductance, and the latter for the analysis of the time structure of the conductance fluctuations. For a change of solution, both the tube and glass beaker were successively rinsed with tap-water, methanol, chloroform and double distilld water, and then oven dried. All water was passed through ion-exchange column and double distilled with all glass still. Measurements were done in symmetrical conditions at room tempreture (23°C±2°C).

4.3 Results

a. Single channel conductance of lysoTPI

In the absence of lysoTPI in the bathing solutions, apparent membrane conductance of oxidized cholesterol or glycerylmonooleate bilayers was approx. 20–50 pS (3–7.5× 10^{-8}S cm^{-2}) in the presence of 500 mM KCl, and no conductance fluctuations were observed at constant voltages below 100 mV. However, upon addition of trace amounts of lysoTPI (approx. 2nM) to the bathing solutions, well defined discrete jumps were frequently observed. Fig. 19a shows the typical conductance fluctuations induced by lysoTPI on an oxidized cholesterol bilayer membrane. The magnituce of the most frequent conductance jumps was approx. 6pS in the presence of 500 mM KCl. Fig. 19b shows the conductance fluctuations induced by lysoTPI on a glycerylmonooleate bilayer membrane. The current fluctuation kinetics were somewhat different from

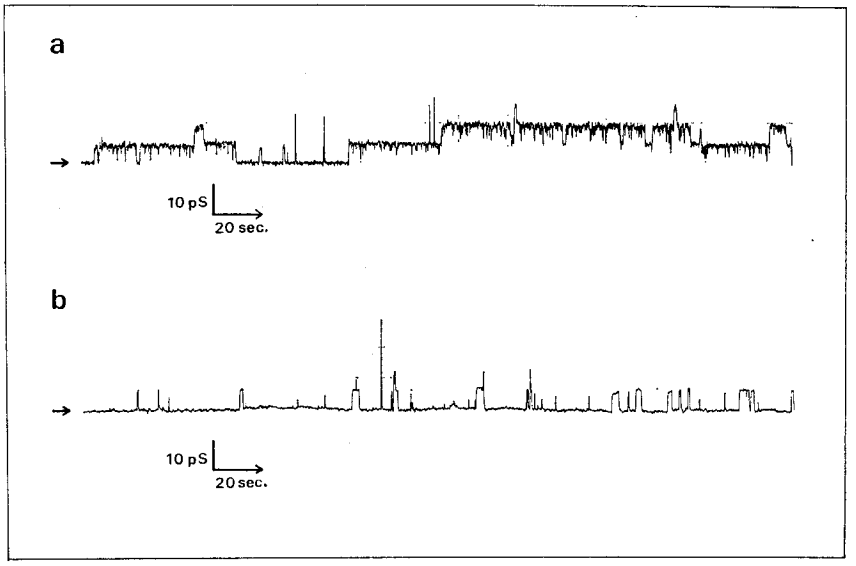

Fig. 19. Conductance fluctuations of lysoTPI channels in (a) oxidized cholesterol and in (b) glycerymonooleate bilayers; electrolytes, 500 mM KCl, 1mM $CaCl_2$, 1 mM Tris-HCl (pH 7.2), 1.6 nM lysoTPI; T=24°C; V=50mV. Horizontal arrow indicates background conductance level. Since fluctuations were recorded with slow-speed recorder (reponse time 1sec.), some short duration jumps were not recorded as full size on the charts.

those in the oxidized cholesterol membrane. However, unit conductance jump was approximately 6pS a value identical to that observed in oxidized cholesterol membranes. Since this magnitude of unit conductance jump is excessively high for a carrier mechanism (Hladky & Haydon, 1972; Läuger, 1972), it is highly likely that lysoTPI forms a channel type structure in both kinds of lipid bilayers. The magnitude of each conductance change was uniform even in multi-step changes as shown in Fig. 19a and b suggesting that the channel had two conductance states corresponding "open" and "closed". Since the height of channel formation step (the first conductance jump after thinning the membrane) was identical to that of the subsequent jumps, the closed state conductance seems much lower than the open state conductance.

Fig. 20 indicates the I-V characteristics of the single channel of lysoTPI in oxidized cholesterol and glycerylmonooleate membranes. Identical linear relationships were obtained on both membranes in the voltage range of 0-125 mV under symmetrical salt condition. At voltages above 100 mV, both kinds of membranes became unstable.

Fig. 21 shows the single channel conductance of lysoTPI as a function of KCl concentration. The single channel conductance appears to approach a limitting value. As a result of this saturating behavior, the dependency of the single channel conduc-

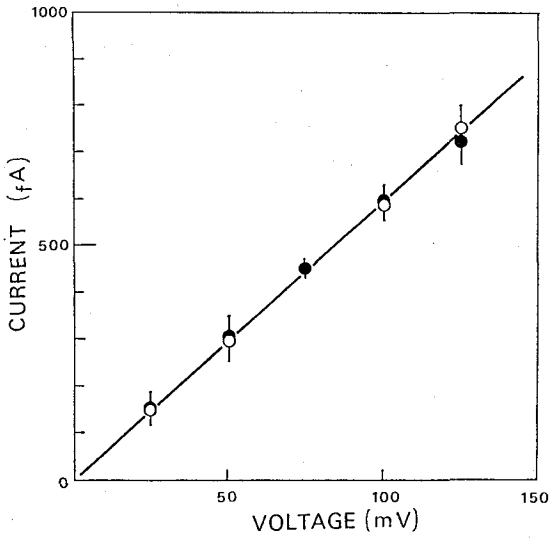

Fig. 20. Steady state current-voltage curves of the single lysoTPI channel in (●) oxidized cholesterol and (o) glycerylmonooleate bilayers in the presence of 500 mM KCl and 10^{-6}M $CaCl_2$. Data represent mean values (±SD) of at least ten events from four membranes.

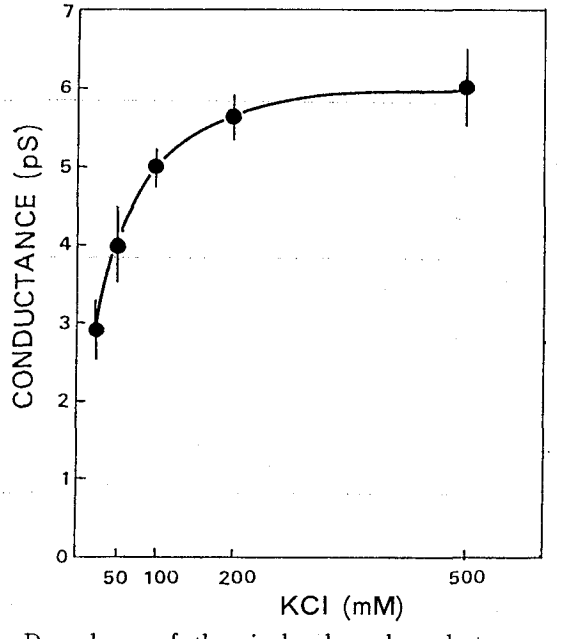

Fig. 21. Dependency of the single channel conductance on KCl concentration in oxidized cholestrol bilayers at 50 mV in the presence of 10^{-6}M $CaCl_2$. Data represent mean values (±SD) of at least five events from three membranes.

tance of lysoTPI on KCl concentration was weaker than that reported for the other ionophores such as EIM or alamethicin (Bean, 1973; Eisenberg et al., 1973) in a middle concentration range of KCl. Similar saturation phenomenon was reported for gramicidin A channel, which was explained in terms of a mutual competition between permeant ions for the binding sites of the channel (Neher et al., 1978). It was expected that the same kind of mechanism assumed for gramicidin A channel limited the rate of ion permeation through lysoTPI channel.

b. Effect of Ca^{++} on the single channel conductance

As mentioned before, small amount of Ca^{++} strongly reduced the univalent cation conductance which was induced by lysoTPI in many-channel membranes. On the other hand, it is known that the single channel conductance of gramicidin A was gradedly reduced and that the I-V curves of it became saturatiing with the increase in the concentration of the divalent cations such as Ca^{++} or Ba^{++} (Bamberg & Läuger, 1977). Thus, it is of special interest to investigate the effect of Ca^{++} on the single channel conductance of lysoTPI. However, as shown in Fig. 22, the size of the single channel conductance of it seems to be unaffected by Ca^{++}. I-V relationships were also unaffected by Ca^{++} concentration in both oxidized cholesterol and glycerylmonooleate membranes (I-V curves were obtained in the concentration range of 10^{-6}–10^{-2}M $CaCl_2$; data were not shown).

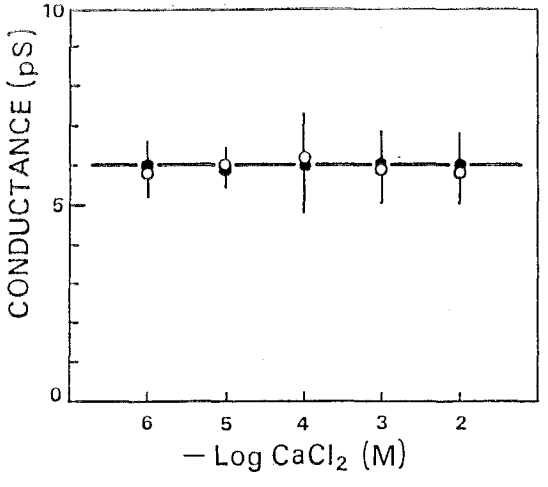

Fig. 22. Single channel conductance as a function of $CaCl_2$ concentration in (●) oxidized cholesterol and in (o) glycerylmonooleate bilayers at 50 mV in the presence of 500 mM KCl.

c. Effect of Ca^{++} on the opening and closing kinetics

Although the single channel conductance of lysoTPI was not affected by Ca^{++}, the kinetics of the opening and closing reaction of lysoTPI channel was affected. To investigate such a Ca^{++}-effect on the conductance fluctuations, a series of experiments was performed in the presence of various concentrations of Ca^{++} with both oxidized cholesterol and glycerylmonooleate membranes. However, in oxidized cholesterol membranes, as a high speed switching reaction occured in the open state of the channel, we could not estimate quantitatively the effect of Ca^{++} on the time structure of conductance fluctuations mainly because of the limited bandwldth of the measuring system. On the other hand, in glycerylmonooleate membranes, the open state of the

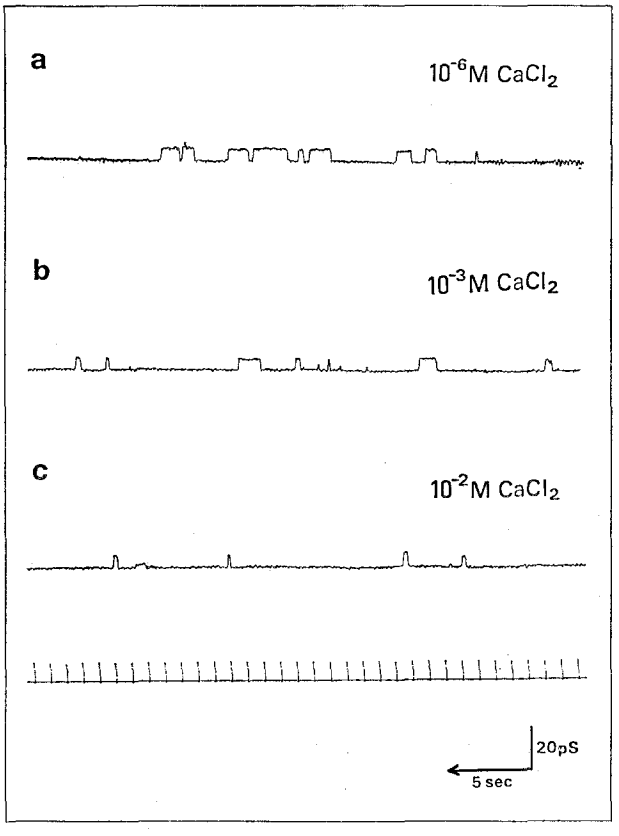

Fig. 23. Conductance fluctuations of the single lysoTPI channel in glycerylmonooleate bilayers at various $CaCl_2$ concentrations; (a) 10^{-6}M, (b) 10^{-3}M, (c) 10^{-2}M, in the presence of 500 mM KCl. Fluctuations were recorded with high speed recorder (response time; 10msec.). A few very small size jumps are seen on the charts, but they were neglected in the statistics shown in Fig. 24. The lowest record is a timing marker.

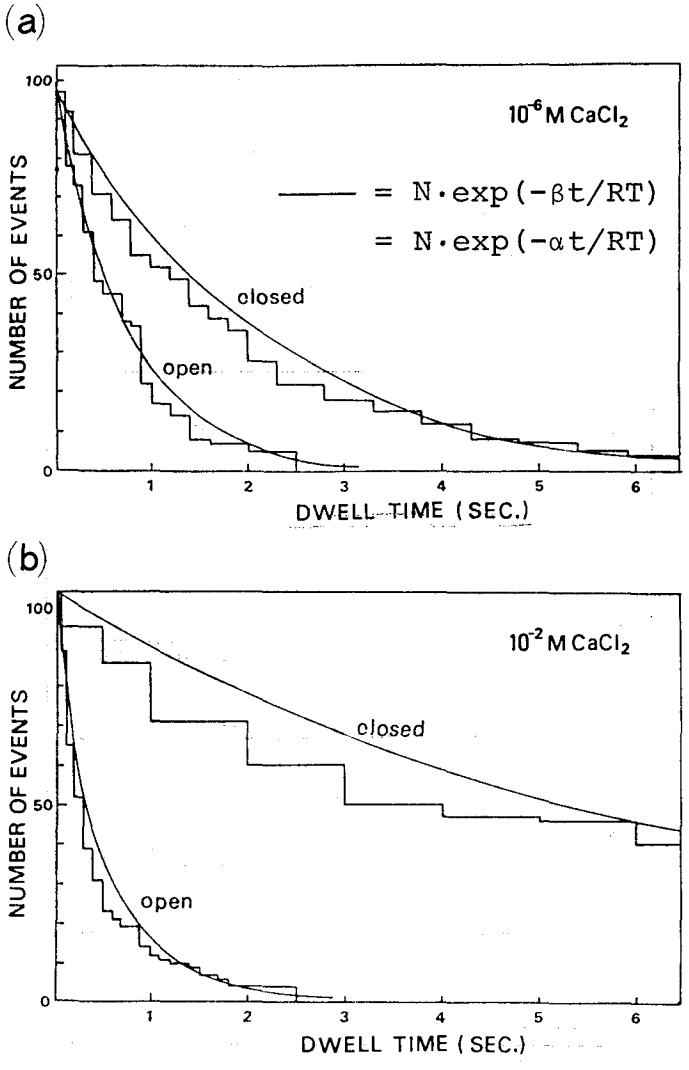

Fig. 24. Distributions of the open and closed dwell times for a single channel in glycerylmonooleate bilayers at (a) 10^{-6}M $CaCl_2$ and (b) 10^{-2}M $CaCl_2$. The number of the individual dwell times which are longer than the time indicated by the abscissa are plotted. The solid curves are single exponential functions ($N\cdot\exp(-\beta t)$, $N\cdot\exp(-\alpha t)$) calculated assmuing that the rate constants were equal to the reciprocal of the averaged dwell times (cf. Eq. 11). N denotes the total number of the events observed.

channel was relatively stable, although the conductance depression by Ca^{++} in many-channel membranes was lesser than that for oxidized cholesterol membranes. Typical effect of Ca^{++} on the current fluctuations in glycerylmonooleate membranes is shown in Fig. 23. Ca^{++} reduced the dwell times for the open state, whereas it increased the dwell times for the closed state. From these data, dwell time histograms were obtained as shown in Fig. 24. The figures show the cumulative sum of the number of events of duration longer than a given dwell time (td) plotted as a function of td. The distribution of the dwell times for both the open and closed states of a single channel was well fitted by a single exponential function as shown in Fig. 24. This fact means that each opening and closing event independently occured on time, i. e., poisson process. This allows us to describe the reaction with the first order kinetics as follows,

$$(\text{closed}) \underset{\beta}{\overset{\alpha}{\rightleftarrows}} (\text{open})$$

where α and β denote the rate constants for the opening and closing of the channel, respectively. α and β are simply the reciprocal of the average dwell time (t_{do}, t_{dc}) for the open and closed states of the channel in the case of first order kinetics (Ehrenstein et al., 1974). That is,

$$\bar{t}_{do} = \frac{1}{m} \sum_{i=1}^{m} t_{doi} = \beta^{-1} \tag{11a}$$

$$\bar{t}_{dc} = \frac{1}{m} \sum_{i=1}^{m} t_{dci} = \alpha^{-1} \tag{11b}$$

where t_{doi} and t_{dci} are individual dwell time for open and closed state, m is the number of jumps in a record. The rate constants calculated from the records on the conductance fluctuations of single-channel membranes at various $CaCl_2$ concentrations are summarised in table 1. It is clear that Ca^{++} decreased α, whereas it increased β. Transition frequency (a numbdr of events per unit time; Pt) defined as

$$Pt = (\bar{t}_{do} + \bar{t}_{dc})^{-1} = \alpha\beta/\alpha + \beta \tag{12}$$

also appears to decrease with Ca^{++} concentration as shown in table 1. Thus, in this scheme, it is suggested that Ca^{++} increased not only a potential energy difference between the open and closed states but also the height of the energy barrier (in this case, activation energy for the opening) between these states.

Effect of Ca^{++} on the conductance of many-channel membranes

Ehrenstein et al. (1974) developed a kinetic theory for the opening and closing of the EIM channels which was able account for the kinetic properties of many-channel membranes. After their theory,we will calculate here the steady state conductance of many-channel membranes using rate constants obtained from the single channel study. The following discussion is based on the assumption that there are no interactions between individual channels.

Let G be a steady state conductance, n_o be the number of the open channel with the conductance g_o, and n_c be that of the closed channel with conductance g_c, then

$$G = n_o g_o + n_c g_c \quad . \tag{13}$$

We consider the membrane having N conducting channels, then

$$N = n_o + n_c \tag{14}$$

stands.

From the principle of detailed balance,

$$\bar{n}_o / \bar{n}_c = \alpha / \beta \tag{15}$$

where the bar denote the equilibrium values.
Combinig Eqs. 13, 14 and 15, we obtain

$$G = N(\alpha g_o + \beta g_c)/(\alpha + \beta) \quad . \tag{16}$$

From the preceeding result, $g_c \ll g_o$ can be assumed, then Eq. 16 becomes

$$G = N g_o \alpha / (\alpha + \beta) \quad . \tag{17}$$

In order to compare the steady state conductnace which was calculated from Eq. 17 with that experimentally obtained, we introduce a relative conductance (Gr) which was defined as a ratio of the conductance at a given concentration of Ca^{++} and that at 10^{-6}M Ca^{++}. Since it could be assumed that both g_o and N were constant under different Ca^{++} concentrations, we obtain

$$Gr = G_j / G_i = \alpha_j (\alpha_i + \beta_i) / \alpha_i (\alpha_j + \beta_j) \tag{18}$$

where the subscripts i and j indicate that the parameters subscripted are at 10^{-6} M

Ca^{++} and at a given Ca^{++} concentration, respectively. Many-channel membrane (100–1000 channels) experiments were carried out with the same procedure as that for few-channel membrane except for the concentration of lysoTPI (see Methods). Calculated and experimental relative conductances are shown in Table 1. The close accordance between two sets of values indicate that, in glycerylmonooleate membranes, the conductance depression by Ca^{++} may principally be explained by the change in the rate constants for the opening and closing reaction of the individual channels.

Table 1 DEPENDENCY OF THE KINETIC PARAMETERS FOR THE OPENING-CLOSING REACTION ON Ca^{++} CONCENTRATION

$CaCl_2$ (M)	Tr (sec.)	n	β^{-1} / α^{-1} (sec.)	β / α (sec.$^{-1}$)	Pt (sec.$^{-1}$)	Calculated Gr	Experimental Gr
10^{-6}	297.6	97	0.81 2.25	1.23 0.44	0.32	1	1
10^{-3}	290.6	55	0.70 4.58	1.43 0.22	0.19	0.48	0.49
10^{-2}	909.6	104	0.56 8.18	1.79 0.12	0.11	0.22	0.25

* Tr, total recording time; n, number of events; β^{-1}, mean open dwell time; α^{-1}, mean closed dwell time; β, rate constant for the closing; α, rate constant for the opening; Pt ($=\alpha \cdot \beta/\alpha+\beta=$ n/Tr), transition frequency ; Calculated Gr, relative conductance calculated by Eq. 18; Experimental Gr, relative conductance of many-channel membrane experimentally obtained.
Data were obtained from at least five membranes.

4.4 Discussion.

a. lysoTPI forms a channel

The conductance of the bilayer membranes modified with a small amount of lysoTPI showed typical discrete conductance jumps of which amplitude was fairly uniform. The height of the most frequent jumps was accounted for 6pS in the presence of 500 mM KCl, this value (10^6 ions/sec, channel) seems to be rather higher than that predicted from a carrier mechanism (Hladky & Haydon, 1972; Läuger, 1972). So, it was assumed that lysoTPI molecule(s) form a pore like structure across bilayer membranes. This idea was supported by another fact that the membrane conductance was induced only when lysoTPI was applied from both sides of the membrane in many-channel membrane system. This fact also suggested that lysoTPI molecules could not be transported from one side of the bilayer membrane to another side, and that the conducting pore unit must be formed by the association of the "half pore" on each side of the membrane as suggested for gramicidin A channel (Bamberg & Janko, 1977; Bamberg & Läuger, 1973, Szabo & Urry, 1978), amphotericin B and

nystatin (Finkelstein & Holz, 1973). Unfortunately, since the conductance dependency as a function of lysoTPI concentration has not yet been determined, how many lysoTPI molecules could form a single conducting channel is unknown. As TPI molecules are known to form a classical micelle in water (Dawson, 1970), lysoTPI could also form a specific micelle in water or in bilayers. It is expected that a number of lysoTPI molecules participate to form a channel.

Yafuso et al. (1974) reported that, in a certain condition, oxidized cholesterol bilayer itself showed discrete conductance jumps (approx. $(5\pm2)\times10^{-10}$S). So, it is possible that the conductance jumps reported here arised from some components in the oxidized cholesterol. However, the fact that the single channel conductance of lysoTPI channel remained constant on both the oxidized cholesterol and glyceryl-monooleate membranes, and that the magnitude of the conductance jumps was much lower than that reported by Yafuso, et al. (1974) indicated that the observed conductance jumps in our study did not arise from some contamination of the bilayer membrane itself. The former fact also suggested that lysoTPI, like EIM or gramicidin, form a pore like structure which may relatively be stable to the change of its surrounding lipid moiety (Bean, 1973; Hladky & Haydon, 1972). Otherwise, this hypothesis was not strictly exact for all cases. Very small (approx. 1-3pS) or very large (approx. 20pS) conductance jumps were also but rarely observed.

b. Does Ca^{++} block the channel?

One of the interesting features of the membranes modified with lysoTPI lies in the fact that the membrane conductance is strongly depressed by Ca^{++}. It was shown that the magnitude of the single channel conductance of lysoTPI channel remained constant to the change of Ca^{++} concentration, whereas the dwell times and the fraction $(\alpha/\alpha+\beta)$ for the open state of the channel were decreased with Ca^{++} concentration. Such a gating by Ca^{++} observed in lysoTPI channel greately differs from the graded blocking of the gramicidin A channel by Ca^{++} (Bamberg & Läuger, 1977), but is similar to the voltage-dependent gating observed in the EIM channel where the dwell times for the open state of the channel were decreased with applied voltages (Alvarez et al., 1975; Ehrenstein et al., 1974).

Here we will describe the reasons why we employed the assumption that Ca^{++} modulated the rate constants of the opening and closing reaction of lysoTPI channel but not that Ca^{++} simply blocked the channel.

1) At free or less than 10^{-6}M Ca^{++}, the time structure of the conductance fluctuations were nearly identical to those at 10^{-6}M Ca^{++}, i. e., lysoTPI channel fluctuated between open and closed states irrespectively of Ca^{++}. In addition, dwell time histograms of the fluctuations at various concentraions of Ca^{++} were well fitted by a single exponential function suggesting that the reaction should be described by the first order kinetics. Thus, it would be more reasonable that Ca^{++} modulated the intrinsic

channel fluctuations than that Ca^{++} induced another reaction such as channel blocking.

2) According to the discussion by Bamberg and Läuger (1977), graded decrease in the single channel conductance might be observed if the transit time (T_t) for the ion permeantion was greater than the time constant (T_b) for the blocking reaction. On the other hand, if T_t was much smaller than T_b, all or none change in the single channel conductance might be recorded. The authors concluded that the former case seemed feasible for gramicidin A channel. If we granted that the latter case occurred in lysoTPI channel, we must then consider the relationship between T_b and the time constant (T_c) for the intrinsic channel fluctuations. If $T_b \ll T_c$, all or none change in the single channel conductance should occur, however, in this case, because of the limitted bandwidth of our current measuring system (10 Hz), we could only observe time averaged blocking reactions, apparently a graded decrease in the single channel conductance. Only in the limitted case $T_b \lesssim T_c$, an all or none conductance change could be observed. However, such a case might hardly occur from physicochemical point of view. It is natural to assume that T_b is smaller than T_c at least by several orders. Thus, it seems difficult to interpret the results shown in Fig. 24 as a channel blocking by Ca^{++}.

3) When channel was blocked by cations, it is suggested that saturating or decreasing I-V curves could be observed (Bamberg and Läuger, 1977; Heckmann et al., 1972). However, as was clearly shown in Fig. 20, the I-V curves of lysoTPI channel were linear irrespectively of Ca^{++}.

Thus, at present, we have no strong indication for the channel blocking by Ca^{++}. These considerations lead us to speculate that lysoTPI channel may have both regulating sites and permeating sites. Ca^{++} might interact with both sites, but more strongly with the former sites. This problem, however, remains to solve.

c. Possible mechanism for the Ca^{++}-effect on channel gating

The difference in Ca^{++}-effect betwèen lysoTPI and gramicidin A channel probably arised from their molecular structure. While gramicidin A has not any ionizable group (Bamberg & Janko, 1977), lysoTPI has three phosphates, and as a result, has five negative net charges per molecule at physiological pH. Moreover, the divalent cations such as Ca^{++} strongly binds to this phosphate moiety resulting in an increase of the hydrophobicity of TPI. Basically a similar hydrophilic-hydrophobic transition by Ca^{++} was observed for an aqueous solution of lysoTPI (unpublished observation). It is highly likely that this hydrophilic-hydrophobic transition for lysoTPI in an aqueous system strongly correlated to the opening-closing transition for the lysoTPI channel state. Many authors representative by Tasaki (1968) have been insisting that the conductance increase associated with nerve excitation arised from hydrophobic-hydrophilic transition of membrane macromolecules. This transition was suggested to be triggered by

the release of membrane bound Ca^{++}. So, it is reasonable to speculate that the closed state for the channel corresponds to the hydrophobic state for the channel and that Ca^{++} stabilized the closed configuration of the channel in lipid bilayers.

As mentioned above, Ca^{++} decreased the transition frequency of the conductance jumps induced by lysoTPI. This means that Ca^{++} increased the height of energy barrier which separates the two configurations of the channel. Some authors interpreted the change of the energy barrier in terms of a change in the fluidity of membrane matrix (Alvarez et al., 1975; Bean, 1973; Ehrenstein & Lecar, 1977). Therefore, Ca^{++} seems to decrease the membrane fluidity to constrain the transition between the two states of lysoTPI channel. This hypothesis is consistent with the recent knowledge that Ca^{++} decreased the fluidity of the lipid bilayers containing acidic lipid (Schnepel et al., 1974; Viret & Leterrier, 1976).

To consider the Ca^{++}-effect on lysoTPI channel further, it is worthwhile to discuss about the origin of the spontaneous conductance fluctuations of lysoTPI channel. There may be at least two possibilities to interpret the spontaneous conductance fluctuations, first that the fluctuations originated from the monomer-dimer reaction between the above mentioned "half pore" on each side of the membrane like as assumed for gramicidine A channel, second that it arised from the spontaneous fluctuations of the structure of the completed lysoTPI channel in bilayer membranes. It can also be speculated that the fluctuations came from the diffusion of the channel from membrane to water or vice versa.. However, as the incorporation of lysoTPI into bilayers occurred irreversibly (cf. S. 3.3 d), the diffusion hypothesis may be neglected here. Recently, we found that, in many-channel membaranes, the effect of Ca^{++} occurred independently on each side of the membrane, namely Ca^{++} on one side of the membrane did not affect the half pore on the other side of the membrane (cf. S. 3.3 b). The total conducatnce was proportional to the product of the fraction of the open state half pore on each side of the membrane (see Fig. 15). From this result, monomer-dimer hypothesis seems most feasible at present. Considering in this line, Ca^{++} might induce a structural change of the half pore to stabilize the monomer form preventing the formation of dimer which corresponds to a conducting channel. However, the mechanism of the Ca^{++}-effect on the half pore has not been resolved. It is known that lysophospholipids have a wedge like (inverted cone) structure to form a spherical micelle and that the structure and the micelle form of it were strongly transformed by Ca^{++} (reviewed by Cullis & Kruijff, 1979). Although it is possible that such a micelle transformation by Ca^{++} may correlate to the Ca^{++}-effect on the half pore, to know the molecular profile of the gating in lysoTPI channel, it should be carried out further studies combining other physichochemical methods.

S. 5 BIOLOGICAL CORRELATES

a. Polyphosphoinositides in acethylcholine receptor membranes

In the previous sections, the evidences that lyso-TPI forms a Ca^{++}-gated univalent cation channel have been shown. However, these results do not immediately mean that lysoTPI forms such a channel in biological membranes. Far from it, there have been no report on the presence of this lipid in biological membranes. Therefore. to substantiate an important role of lysoTPI in the control of the ionic permeability of bilogical membranes, we must at least answer the following questions: "Is there lyso-TPI in excitable membranes ?" and "Is lysoTPI responsible to the stimulus-response coupling during excitation ?". The first problem does not seem so difficult, but to answer the second question seems much difficult because of the high complexity of usuall membranes. Therefore, to avoid the difficulties in the interpretation of the experimental results, we must carefully choose the membrane sample which has the most simplified system for the excitation.

We employed acethylcholine receptor (Ach R) membranes purified from electroplax of *Narke Japonica* as the excitable membranes. The AchR is the most commonly purified receptor protein which has specific Ach binding sites and at the same time, a channel mechanism controlled by the former. This may be the simplest system which keeps excitability, therefore the ideal sample for our purpose. Recently, it has become relatively easy to obtain AchR membranes of high purity by alkaline-treatment. We studied the effects of an agonist, carbamylcholine on ^{32}p-incorporation by the phospholipids of alkaline-treated AchR membranes. In Na^+-rich medium, carbamyl-choline drastically activated the labelling of two substances which seemed to be lysoPPI. On the other hand, in K^+-rich medium, TPI incorporated ^{32}P although no carbamyl-choline effect was obtained in this case. The typical results are shown in Fig. 25 (Hayashi, Sokabe, & Amakawa 1981a).

It is noteworthy that, in the Na^+-medium, carbamylcholine remarkably enhanced the phosphorylation of the two substances which gave two distinct bands below TPI on HPTLC. We have recently found that autoxidation products of purified PPI ex-tracted from bovine brain gave the same bands on HPTLC as the two radioactive bands induced by carbamylcholine in the AchR membranes (unpublished). It is well known that autoxidation of highly unsaturated phospholipids brings about the formation of lyso-like phospholipids and short acyl chain (May & McCay, 1968). Taking into the fact that PPI have an arachidonic acid at β-position (Holub et al., 1970), the two components which were induced by carbamylcholine seemed to be lysophospholipids produced from PPI.

Fast occurrence of lipid peroxidation following stimulus reception on bilogical membranes has been reported (Kagan et al., 1973). The presence of highly unsatura-ted fatty acid especially docosahexaenoic acid ($C_{22:6}$) characterizes the fatty acid

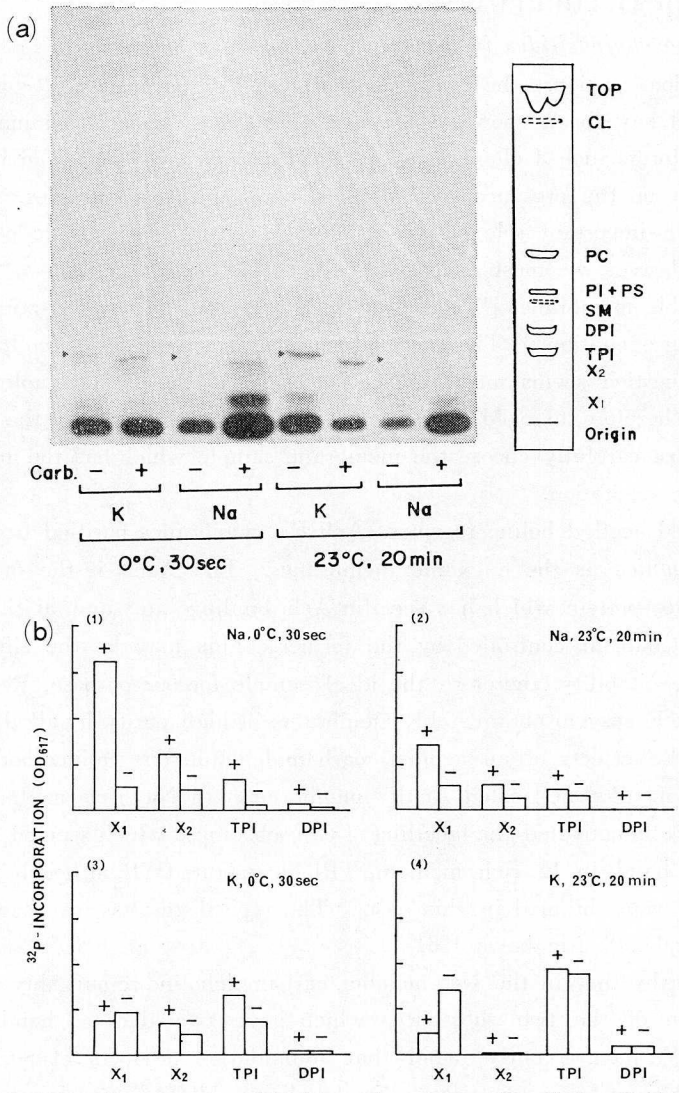

Fig. 25. (a) Autoradiogram after thin layer chromatography of phospholipids from acethylcholine receptor membranes. The membranes were labeled with [γ-^{32}P]ATP in different conditions as indicated. Carb. "+" and "−" indicate presence and absence of carbamylcholine (10^{-6}M) in reaction medium, respectively. "Na" and ,'K" mean 0.1 M of Na^+ and K^+ in the medium, respectively. Right hand side column illustrates phospholipids visualized by I_2 vapor. Trace spots are shown in dotted lines. Purified DPI and TPI were added as a carrier. Triangles mark position of TPI. CL, caldiolipin; PC, phosphatidylcholine; PI, phosphatidylinositol; PS, phosphatidylserine; SM, sphingomyeline ; DPI, diphosphoinositide; TPI, triphosphoinositide; X_1 and X_2, lysopolyphosphoinositides. (b) Carbamylcholine induction of dynamic changes in the phsophorylation of polyphosphoinositides from acethylcholine receptor membranes. Symbols, the same as in (a).
(Hayashi et al., 1981a)

composition in synaptic plasma membranes as well as the rod outer segment of retina (Daemen, 1973; Wheeler et al., 1975)). Therefore, it was suggested that carbamylcholine induced the fast lipid peroxidation in the AchR membranes. However, there is no evedence to exclude the contribution of phospholipase A_2 activity to the lysoPPI production. Recently, we observed a similar metabolic change of lysoPPI by photic stimulation in the disc membranes from rod outer segment of frog retina (Hayashi, Sokabe & Amakawa, 1981b).

b. Polyphosphoinositides in Paramecium

More recently, to confirm the physiological role of PPI and lysoPPI in biological membranes we employed a new strategy where protozoa mutants that genetically lack nomal ion channels were used. *Paramecium tetraurelia* mutants are unusually useful subjects for that study, because many behavioral mutants were well documented, and its correlation with the ion channel-deficit was also well established by electrophysiology (reviewed by Cronkite, 1979). We used three types of mutants, *pawn*, *fast*, and *TEA-insensitive* together with *wild* type as a control.

^{32}P incorporation by PPI or lysoPPI were distinctive among these species. Most interesting result was obtained in the *fast* type mutants whose K^+-channel was suggested to have an increased permeability to K^+ compared with that of *wild* type (Satow & Kuhn, 1976). Rapid and strong ^{32}P incorporation by PPI and lysoPPI was found in the cilia and deciliated body fraction from the *fast* type mutants (Sokabe et al., in preparation). This gave a strong support for the correlation between lysoPPI and K^+-channel in the membranes of *fast* type mutants because any other membrane components distinctive from wild type have not been reported.

Thus, some evidences that suggest the importance of lysoTPI for ion permeation

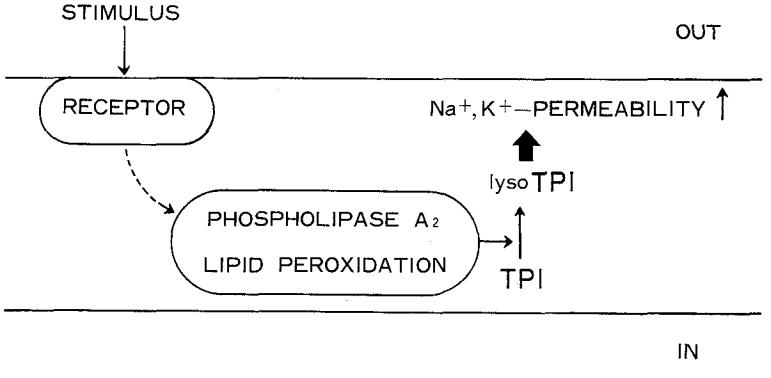

Fig. 26. Possible control of membrane permeability by lysoTPI. After stimulus reception, activation of phospholipase A_2 or lipid peroxidation through unknown passway (indicated by broken line) occurred to produce lysoTPI.

across biological membranes have been accumulated. For the future work, we propose here a prelimirary hypothesis schematized in Fig. 26, where a stimulus-driven metabolic chain which could produce lysoTPI is introduced. Hereafter, more works should be done to verify this hypothesis using many other excitable membranes.

c. Polyphosphoinositides and drug reception.

Finally, we comment on the possibility that PPI may take part not only in ion permeation but also in drug reception. Aminoglycoside antibiotics such as streptomycin, neomycin etc. are well known for their strong ototoxic action. Direct administration of these drugs to the inner ear brings about a rapid reduction of the chochlear microphonic potentials that arised from the receptor potential of hair cells (Lohdi et al., 1980). It is also well known that neomycin inhibited PPI metabolism in vivo and vitro (Schacht, 1978). Based on these results, it was suggested that PPI might be a primary receptor for these antibiotics, and that PPI might participate in the electric phenomena in the inner ear (Schacht, 1976).

Using artificial bilayer lipid membranes, we recently found that several aminoglycosides strongly blocked lysoTPI channel, and that the power of the blocking action among drugs was pararelled by the ototoxicity (Sokabe, Hayase and Miyamoto, 1982). It is also found that aminopyridine a specific K^+-channel blocker appreciably blocked lysoTPI channel (unpublished).

In this way, lysoTPI can offer a useful model for the study of molecular events occurred in excitable membranes. It is our dream, combining artificial bilayer lipid membranes and bilogical membranes, to clarify the molecular mechanism of the change in the ionic permeability during excitation based on a PPI metabolism.

SUMMARY

TPI is quantitatively a minor but metabolically an active component of various plasma membranes, and has a high affinity for Ca^{++}. Owing these unique properties, TPI has been speculated to have an important role in the control of ionic permeability of excitable membranes. However, there is no direct evidence that this lipid participates in membrane functions.

We tried to check the possibility whether TPI affects the membrane permeability by incorporating this lipid into artificial bilayer lipid membranes. Consequently, it was found that lysoTPI an autoxidized product of TPI could successfully form a stable cation permeable channel. This channel selectively permeated univalent cations, but was inhibited by a small amounts of divalent cations such as Ca^{++}. In this report, we centered our interest on the physicochemical mechanism of this conductance inhibition by Ca^{++}.

In macroscopic experiments, it was comfirmed that Ca^{++} inhibited the K^+-conductance of lysoTPI channel in a competitive manner, and that the change in surface potential

had a little contribution to the conductance inhibition. In microscopic (single channel) experiments, it was suggested that Ca^{++} gated the channel resulting in a decrease in the opening dwell times rather than a blocking mechanism. Thus, we could obtain a evidence that lysoTPI could form a Ca^{++}-gated univalent cation channel in bilayer lipid membranes. This channel was also sensitive to aminoglycosides and aminopyridines which are known to block the ionic channel in nerve membranes. However, the exsistence of lysoTPI and its physiological role in biomembranes have been completely unknown.

Preliminary studies on these problems were carried out by using some biological membranes. In acethylcholine receptor membranes, we found lysoPPI of which phosphorylation was increased by carbamylcholine one of the potent agonists to acethylcholine receptor. In addition, a transient enhancement of ^{32}p incorporation by lysoTPI by photic stimulation was observed in the disc membranes from frog rod outer segment.

Based on these results, it was suggested that the reactions (lipidperoxidation or phospholipase activation) that could produce lysoTPI have a key role in the molecular events during the excitation of biomembranes.

ACKNOWLEDGEMENT

At first, the author wish to express his hearty thanks to collegue Dr. F. Hayashi. Most of the data presented in this report were obtained with his collaboration. Thanks are also due to Profs. R. Suzuki, U. Kishimoto, K. Miyamoto, M. Takagi, K. Hayashi, and Dr. T. Amakawa for their discussion and encouragement. This work was supported in part by Sakkokai Foundation and the grant 579157 from the Ministry of Education.

REFERENCES

Abdel-Latif, A. A., K. K. Green, J. P. Smith, J. C. Mcpherson, Jr., and J. L. Matheny 1978. Norepinephrin-stimulated break down of triphosphoinositide of rabbit iris smooth muscle: effect of surgical sympathetic denervation and in vivo electrical stimulation of the sympathetic nerve of the eye. *J. Neurochem.* **30**: 517-525.

Alvarez, O., R. Latorre, and P. Verdugo 1975. Kinetic characterisics of the excitability -inducing material channel in oxidized cholesterol and brain lipid bilayer membranes. *J. Gen. Physiol.* **65**: 421-439.

Bamberg, E., and P. Läuger. 1973. Channel formation kinetics of gramicidin A in lipid bilayer membranes. *J. Memb. Biol.* **11**: 177-194.

Bamberg, E., and P. Läuger. 1977. Blocking of the gramicidin channel by divalent cation. *J. Memb. Biol.* **35**: 351-375.

Bamberg, E., and K. Janko. 1977. The action of a carbonsuboxide dimelized gramicidin A on lipid bilayer membranes. *Biochim Biophys. Acta.* **465**: 486-499.

Bartlett, G. R. 1959. Phosphorus assay in column chromatography. *J. Biol. Chem.* **234**: 466-468.

Bean, R. C., 1973. Protein-mediated mechanism of variable ion conductance in thin lipid membranes. *In* Membranes: A Series of Advances. G. Eisenman, editor. Marcel Dekker Inc., N. Y. Vol 3: 409-477.

Birnberger, A. C., K. L. Birnberger, S. C. Eliasson, and P. C. Simpson. 1971. Effect of cyanide and electrical stimulation on phosphoinositide metabolism in lobster nerves. *J. Neurochem.* **18**: 1291-1298.

Brockerhoff, H., and C. E. Ballou. 1962. Phosphate incorporation in brain phosphoinositides. *J. Biol. Chem.* **237**: 49-52.

Cronkite, D. L., 1979. The genetics of swimming and mating behavior in *Parameciu*m. *In* Biochemistry and Physiology of Protozoa. Academic press N. Y.: 221-273.

Cullis. P. R., and B. De Kruijff. 1979. Lipid polymorphism and the functional roles of lipids in biological membranes. *Biochim. Biophys. Acta.* **559**: 339-420.

Daemen, F. J. M., 1973. Vertebrate rod outer segment membranes. *Biochim. Biophys. Acta.* **300**: 255-288.

Dawson, R. M. C. 1969. Metabolism and function of polyphosphoinositides in nervous tissue. *Ann. N. Y. Acad. Sci.* **165**: 774-783.

Dawson, R. M. C., and H. Hauser. 1970. Binding of calcium to phospholipids. *In* Calcium and Cellular Function. Cuthberd, editor, Macmillan Publising Co. Inc., Riverside Newjersey. 17-41.

Eisenberg, M., J. E. Hall, and C. A. Mead. 1973. The nature of the voltage-dependent conudctance induced by alamethicin in black lipid membranes. *J. Memb. Biol.* **14**: 143-176.

Ehrenstein, G., R. Blumenthal, R. Latorre, and H. Lecar. 1974. Kinetics of the opening and closing of individual excitability inducing material channels in lipid bilayer. *J. Gen. Physiol.* **63**: 707-721.

Ehrenstein, G., and H. Lecar. 1977. Electrically gated ionic channels in lipid bilayers. *Quart. Rev. Biophys.* **10**: 1-34.

Finkelstein, A., and R. Holz. 1973. Aqueous pores created in thin lipid membranes by the polyene antibiotics nystatin and amphotericin B. *In* Membranes: A Series of Advances. G. Eisenman, editor. Marcel Dekker Inc., N. Y. Vol. **3**: 377-408.

Fishman, S. N., B. I. Chodorov, and M. V. Volkenstein., 1971. Molecular mechanism of membrane ionic permeability. *Biochim. Biophys. Acta.* **225**: 1-10.

Frankenhaeuser, B. and A. L. Hodgkin., 1957. The action of calcium on the electrical properties of squid axon. *J. Physiol.* **137**: 218-244.

Gilbert, D. L., and G. Ehrenstein. 1969. Effect of divalent cations on potassiun conductance of spuid axons. *Biophys. J.* **9**: 447-464.

Gotoh, H., 1975. A model of the activation process of Na^+ conductance in the squid axon: an approach with interactive desorption kinetics of divalent cations. *J. Theor. Biol.* **53**: 309-325.

Graham, D. C., 1947. The electrical double layer and the theory of electrocapillarity. *Chem. Rev.* **41**: 441-501.

Greengard, P. and J. W. Kebabian., 1974. Role of cyclic AMP in synaptic transmittion in the mammalian peripheral nervous system. *Fed. Proc.* **33**: 1059-1067.

Hagiwara, S., D. C. Eaton, A. E. Stuart, and N. P. Rosenthal. 1972. Cation selectivity of the resting membrane of squid axon. *J. Memb. Biol.* **9**: 373-384.

Hayashi, F., M. Sokabe, K. Hayashi, M. Takagi, and U. Kishimoto. 1978. Calcium sensitive univalent cation channel formed by lysotriphosphoinositide in bilayer lipid membranes. *Biochim. Biophys. Acta.* **510**: 305-315.

Hayashi, F. and M Sokabe. 1978. Calcium sensitive univalent cation channel made of lysotriphosphoinositide in planar bilayer membranes. *Sixth Int. Biophys. Cong. Abs.*: 143p.

Hayashi, F., M. Sokabe, and T. Amakawa. 1981a. Carbamylcholine effect on inositol phospholipids in acethylcholine receptor membranes from *Narke japonica.* Proc. Jap. Acad. **57B**: 48-53.

Hayashi, F., M. Sokabe, and T. Amakawa. 1981b. Inositol phospholipids in frog rod outer segment. *19th Ann. Met.Jap. Biophys. Soc.*

Hawthorn, J. N. and D. A. White. 1975. Myo-inositol lipids. *Vitamins & Hormons.* **33**: 529-573.

Heckmann, K., B. Lindemann, and J. Schnakenberg. 1972. Current-voltoge curves of porous membranes in the presence of pore -blocking ions. I. Narrow pores containing no more than one moving ion. *Biophys. J.* **12**: 683-702.

Hendrickson, H. S. 1969. Physical properties and interactions of phosphoinositide. *Ann. N. Y. Acad. Sci.* **165**: 668-676.

Hendrickson, H. S., and C. E. Ballou. 1964. Ion exchange chromatography of intact brain phosphoinositides on diethylaminoethyl cellulose by gradient salt elution in a mixed solvent system. *J. Biol. Chem.* **239**: 1369-1373.

Hendrickson, H. S. and J. G. Fullington. 1965. Stabities of metal complexes of phospholipids: Ca (II), Mg (II) and Ni (II) complexes phosphatidylserine and triphosphoinositide. *Biochemistry* **4**: 1599-1605.

Hendrickson, H. S., and J. L. Reinertsen. 1971. Phosphoinositide interconversion: a model for control of Na^+ and K^+ permeability in the nerve axon membrane. *Biochem. Biophys. Res. Commun.* **44**: 1258-1264.

Hladky, S. B., and D. A. Haydon. 1972. Ion transfer across lipid membranes in the presence of gramicidin A. *Biochim. Biophys. Acta.* **274**: 294-312.

Holub, B. J. 1970. Moleular species of mono-, di- amd triphosphoinositides of bovine brain. *J. Lipid Res.* **11**: 558-564.

Jolles, J., K. W. A. Wirtz, P. Schotman, and W. H. Gipsen. 1979. Pituitary hormones influence polyphosphoinositides metabolism in rat brain. *FEBS Letters.* **105**: 110-114.

Kagan, V. E., A. A. Shvedova, K. N. Novikov, and Yu. P. Kozlov. 1973. Light induced free radical oxidation of membrane lipids in photoreceptor of frog retina. *Biochim. Biophys. Acta.* **330**: 76-79.

Kai, M., and J H. Hawthorn. 1969. Physiological significance of polyphosphoinositides in brain. *Ann. N. Y. Acad. Sci.* **165**: 761-773.

Läuger, P. 1972. Carrier-mediated ion transport. *Science.* **178**: 24-30.

Lee, Y. and S. I. Chan. 1977. Effect of lysolecithin on the structure and permeability of lecithin bilayer vesicle. *Biochemistry.* **16**: 1303-1309.

Lohdi, S., N. D. Weiner, I. Mechigian, and J. Schacht, 1980. Ototoxicity of aminoglycosides correlated with their action on monomolecular films of polyphosphoinosotides. *Biochem. Pharmacol.* **29**: 597-601.

May, H. E. and P. B. McCay. 1968. Reduced triphosphopyridine nucleotide oxidase-catalyzed alterations of membrane phospholipids. *J. Biol. Chem.* **243**: 2288-2295.

McLaughlin, S. G. A., G. Szabo, G. Eisenman, and S. M. Ciani. 1970. Surface charge and the conductance of phospholipid membranes. *Proc. Natl. Acad. Sci. U. S. A.* **67**: 1268-1275.

McLaughlin, S. G. A., G. Szabo, and G. Eisenman. 1971. Divalent ions and the surface potential of charged phospholipid membranes. *J. Gen. Physiol.* **58**: 667-687.

Michell, R. H. 1975. Inositol phospholipids and cell surface receptor function. *Bichim. Biophys. Acta* **415**: 81-147.

Michell, R. H. 1979. Inositol phospholipids in membrane function. *Trends Biochem. Sci.* **4**: 128-131.

Miller, C. 1978. Voltage-gated cation conductance channel from fragmented sarcoplamic reticulum; steady state electrical properties. *J. Memb. Biol.* **40**: 1-23.

Nachmansohn, D. and E. Neuman. 1975. Chemical and Molecular Basis of Nerve Activity. Academic press N. Y.

Neher, E., J. Sandblom, and G. Eisenman. 1978. Ionic selectivity saturation and block in gramicidin A channels II: saturation behavior of single channel conductances and evidence for the existence of multiple binding sites in the channel. *J. Memb. Biol.* **40**: 97-116.

Neuman, E. 1973. An integral physico-chemical model for bioexcitability. *In* Physics and Mathematics of The Nervous System. Conrad, M., W. Guttinger, and M. Dal Cin, editors. Springer-Verlag Berlin.: 42-81

Oliveira-Castro, G. M. and W. R. Loewenstein. 1971. Junctional membrane permeability — Effect of divalent cations —. *J. Memb. Biol.* **5**: 51-77.

Robinson, R. L., and A. Strickholm. 1978. Oxidized cholesterol bilayers: dependence of electrical properties on degrade of oxidation and aging. *Biochim. Biophys. Acta.* **509**: 9-20.

Rose, B., I. Simpson, and W. R. Loewenstein. 1977. Calcium ion produces graded change in permeablity of membrane channel in cell junction. *Nature.* **267**: 625-627.

Satow, Y. and C. Kuhn. 1976. A mutant of paramecium with increased relative resting potassium permeability. *J. Neurobiol.* **7**: 325-338.

Schacht, J. Biochemistry of neomycin ototoxicity. *J. Acoust. Soc. Am.* **59**: 940-944.

Schacht, J. 1978. Interaction of aminocyclitol antibiotics in mammalian tissues and artificial membranes. *In* Cyclitols and Phosphoinositides. Wells, W. W. and F. Eisenberg, editors. Academic Press N. Y.: 153-165.

Schnepel, G. H., D. Hegner, and U. Shummer. 1974. The influence of calcium on the molecular mobility of fatty acid spin labels in phosphatidylserine and phosphatidylinositol structures. *Biochim. Biophys. Acta.* **367**: 67-74.

Snyder, F. and N. Stephens. 1959. A simplified spectrophotometric determination of ester groups in lipids. *Biochim. Biophys. Acta* **34**: 244-245.

Sokabe, M. 1975. Cation channel induced by lysotriphosphoinositide. *Master thesis* Fac. Engineering Sci. Osaka Univ.

Sokabe, M. and F. Hayashi. F. 1978. Ion channel formed from biomolecules in bilayer model membranes. (in japanese). *Tec. Rep. Jap. IECE.* **MBE 78-9**: 11-22.

Sokabe, M. and F. Hayashi. 1981a. Ca^{++}-effect on the K^+-conductance of the bilayer membranes modified by lysotriphosphoinositide. (submitted)

Sokabe, M. and F. Hayashi. 1981b. Unit conductance channel of lysotriphosphoinositide. *Biophys. J.* (to be published).

Sokabe, M., J. Hayase, and K. Miyamoto. 1982. Effects of neomycin on the K^+-permeability of the bilayer lipid membranes modified with lysotriphospoinositide: a model for the neomycin ototoxicity. *Neurosci. Let.* (in press).

Szabo, G., and D. W. Urry. 1978. N-acethyl gramicidin : single channel properties and implications for channel structure. *Nature.* **203**: 55-57.

Tasaki, I. 1968. Nerve excitation: a macromolecular approach. C. C. Thomas Pub. Springfield Illinois U. S. A.

Torda, C. 1974. Model of molecular mechanism able to generate a depolarization-hyperpolarization cycle. *In* International Review of Neurobiology, Pfeiffer, C. and J. R. Smythies, editors, Academic Press, N. Y. Vol 16: 1-66.

Tret'jak, A. G., I. M. Limarenko, G. V. Kossava, P. V. GuLak, and Yu. P. Kozlov. 1977. Interrelation of phosphoinositide metabolism and ion transport in crab nerve fibers. *J. Neurochem.* **28**: 199-205.

Viret, J., and F. Leterrier. 1976. A spin label study of rat brain membranes: effects of tempreture and divalent cations. *Biochim. Biophys. Acta.* **436**: 811-824.

Wheeler, T. C., R. M. Benolken and R. E. Anderson. 1975. Visual membranes: specifity of fatty acid precursors for the electrical response to illumination. *Science.* **188**: 1312-1314.

Yafuso, M., S. J. Kennedy, and A. R. Freeman. 1974. Spontaneous conductance changes: multilevel conductance states and negative differential resistance in oxidized cholesterol black lipid membranes. *J. Memb. Biol.* **17**: 201-212.